Journal of Advanced Ceramics
2021, **10**(1): 1–27
https://doi.org/10.1007/s40145-020-0422-5
ISSN 2226-4108
CN 10-1154/TQ

Review

Micro-fabrication of ceramics: Additive manufacturing and conventional technologies

Hany HASSANIN[a,*], Khamis ESSA[b], Amr ELSHAER[c], Mohamed IMBABY[d,e], Heba H. EL-MONGY[d,f], Tamer A. EL-SAYED[d,f]

[a]*School of Engineering, Canterbury Christ Church University, Canterbury, CT1 1QU, UK*
[b]*University of Birmingham, Edgbaston, B15 2TT, UK*
[c]*Kingston University London, Penrhyn Road, Kingston Upon Thames, Surrey, KT1 2EE, UK*
[d]*Department of Mechanical Design, Faculty of Engineering, Mataria, Helwan University, P. O. Box. 11718, Cairo, Egypt*
[e]*Jubail University College, Mechanical Engineering, Kingdom of Saudi Arabia*
[f]*Center for Applied Dynamics Research (CADR), School of Engineering, University of Aberdeen, Aberdeen, AB24 3UE, UK*

Received: June 7, 2020; Revised: August 31, 2020; Accepted: September 9, 2020

Abstract: Ceramic materials are increasingly used in micro-electro-mechanical systems (MEMS) as they offer many advantages such as high-temperature resistance, high wear resistance, low density, and favourable mechanical and chemical properties at elevated temperature. However, with the emerging of additive manufacturing, the use of ceramics for functional and structural MEMS raises new opportunities and challenges. This paper provides an extensive review of the manufacturing processes used for ceramic-based MEMS, including additive and conventional manufacturing technologies. The review covers the micro-fabrication techniques of ceramics with the focus on their operating principles, main features, and processed materials. Challenges that need to be addressed in applying additive technologies in MEMS include ceramic printing on wafers, post-processing at the micro-level, resolution, and quality control. The paper also sheds light on the new possibilities of ceramic additive micro-fabrication and their potential applications, which indicates a promising future.

Keywords: micro-electro-mechanical system (MEMS); micro-fabrication; ceramics; micro parts; additive manufacturing

1 Introduction

The increasing demand for micro-fabrication technologies has prompted the introduction of novel miniaturised devices such as sensors, accelerometers, drug delivery systems, 3D printers, micro-mirrors, wireless electronics, blood analysers, and micro-heat exchangers. As a result, the global MEMS market has increased from \$11.7 billion in 2014 to \$21.9 billion in 2020 [1]. Historically, Feynman [2] presented MEMS technology in his presentation titled "There is plenty of room at

* Corresponding author.
E-mail: enghanisalama@yahoo.com

the bottom" in 1959. Following this, Petersen [3] introduced silicon as a promising material for the fabrication of micro-components which is the basis of the current MEMS technology. During the 1990s, MEMS technologies were developed further as a result of the introduction of the integrated circuit (IC). Since then, researchers have been actively interested in developing MEMS technologies [4]. This is shown in the increased published journal papers on using microfabrication/ MEMS over the past twenty years (see Fig. 1). The published journal papers exhibited an increase from 1000 papers a year in 1999 to over 5500 papers a year in 2007. Since then, the publication output has stabilised to an average of 5000 papers per year.

Material choice has a significant effect on MEMS system performance. Mechanical, physical, thermal, electrical, as well as corrosion resistance are essential to be defined before choosing the appropriate material. Silicon and polymer-based materials have been widely implemented in MEMS because they have favourable processing and functional properties [5,6]. On the other hand, ceramic materials offer a suitable solution to provide a specific functionality or fabrication simplicity. Ceramics are chemically inert which can be used in biological devices. The high service temperature and low density of ceramics allow them to be used in high-speed devices such as micro-engines and micro-turbines. They are also resistant to corrosion at high temperature, making them meet the chemical micro-sensing requirements. The wear resistance makes them ideal materials in moving systems to overcome the developed friction of high micro-motorised devices. Furthermore, although ceramics are sensitive to flaws, their mechanical properties and reliability are expected to improve at the micro-nano scale.

Micro-fabrication techniques have been advanced throughout the past 30 years, but most of the progress has been focused on developing new MEMS with

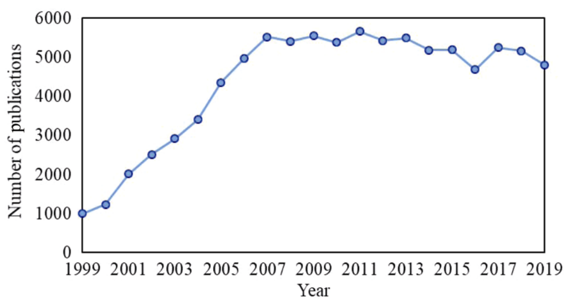

Fig. 1 Number of published papers about microfabrication over the last 20 years.

intricate designs with high precision [7]. Besides, the performance of MEMS may be degraded by dust particles, and special manufacturing environments such as cleanrooms are needed to produce high-quality MEMS. Therefore, there is a demand to employ simple manufacturing techniques, which can produce complex-shaped three-dimensional geometries with high aspect ratios. Three-dimensional (3D) micro-components with complex geometries play an important role in advanced MEMS such as microfluidic devices, biochips, photonic crystals, and many others. MEMS industry will be progressed substantially if complex-shaped 3D geometries can be fabricated and integrated to high-performance devices and assemblies. Several conventional manufacturing technologies have been introduced to produce 3D ceramic micro-components. However, the majority of the conventional micro-fabrication processes has the ability to produce 2.5D ceramic micro-parts and does not have the aptitude to fabricate true 3D micro-parts. Emerging technologies such as additive manufacturing have been investigated to improve the capabilities of MEMS industry to fabricate complex-shaped 3D micro-components. There is a lacking in reviewing the current progress of using advanced technologies such as additive manufacturing in ceramic MEMS industry. This paper explores the use of advanced ceramic micro-fabrication techniques with an emphasis on additive manufacturing. The paper gives a comprehensive overview of the micro-fabrication processes used for ceramic structures showing their working principles, materials, applications, and limitations.

2 MEMS ceramic materials

Ceramic materials are typically used in the fabrication processes of MEMS to provide additional property, performance, functionality, or fabrication simplicity. High-temperature resistance ceramics are used in applications such as micro heaters, high-temperature sensors, micro-engines, micro-fuel cells, piezoelectric energy harvesters, micro-needles, and micro-electrochemical sensors [8–16]. Most of the conventional and additive micro-manufacturing processes of ceramic MEMS are based on the advancement in colloidal powder processing science prior to shaping and sintering. Therefore, understanding the particle-to-particle interaction remains a critical key to the successful realisation of adequate ceramic suspension, paste, or slurry used in conventional or additive micro-fabrication techniques. Figure 2 shows the different inter-particle attraction action forces between ceramic particles. Ceramic suspensions can be controlled depending on the addition of additives from highly dispersed to weakly flocculated particles [17,18]. Electrostatic, steric, and electro-steric stabilisation are the three different mechanisms to disperse ceramic powders in solutions. Ceramic suspensions become highly dispersed when the repulsion forces are high. To prepare highly dispersed suspensions with high solid loading, electro-steric stabilisation is typically used by the addition of polyelectrolyte species, which contain ionisable functional group. Strong adsorption between polyelectrolyte and the ceramic particles is expected when they have opposite surface charges. On one hand, steric stabilisation is typically used in non-aqueous suspensions at which the adsorbed molecules produce steric repulsion to prevent ceramic powders from being agglomerated. High solid loading and low viscosity with long-term stability are important rheological properties that should be considered during the preparation of ceramic suspensions or slurries. In particular, the effects of suspension additives such as dispersant concentration, type, and solid loading on the rheological and dispersion behaviour of the ceramic slurries play a vital role on the properties of the fabricated ceramic parts. A chemical reaction is created between ceramic particles and the dispersant. In addition, anchor groups are adsorbed on the surface of ceramic particle surface as well as solvent chains are developed and formed steric layer [19–21].

On the other hand, it is highly important to minimise part shrinkage due to drying, de-binding, and sintering

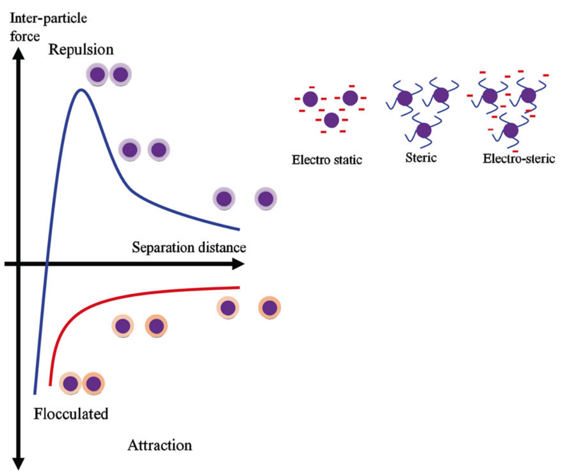

Fig. 2 Schematic diagram of the inter-particle interactions and forces between ceramic particles.

in order to achieve dense and crack free components. To minimise shrinkage, highly solid loading and small particle size with minimal additives are typically used in the preparation of ceramic suspensions. Furthermore, using ceramic suspensions with minimum additives facilitates the de-binding process and minimises the potential of forming cracks [22].

Co-fired ceramics are ceramic micro-electronic systems where dielectric materials, conductors, and ceramic substrates are sintered in a high-temperature furnace simultaneously. The technology of co-fired ceramics is widely used for high-temperature MEMS as well as in MEMS packaging applications. Low-temperature-co-fired-ceramic (LTCC) are typically sintered at a temperature below 1000 ℃ through the addition of glassy-phase materials with low melting temperature to the ceramic. Several research groups used LTCC ceramic in the fabrication of micro hot plates [16,23,24]. An increase in the operating temperature of MEMS is achievable by using refractory ceramics. Alumina and zirconia are the two oxide ceramics used in micro-fabrication of high-temperature resistance MEMS. Iovdalskiy *et al.* [25] are one of the first researchers to invent a technique to produce a micro-heater using alumina. The main advantage of using a substrate made of alumina in micro-heaters compared to silicon-based materials is the excellent bonding between platinum and alumina at a wide range of high temperatures without the need of using adhesives. The platinum-coated alumina substrate remained stable and intact after heating at 850–1000 ℃, and it worked at 600 ℃ for several years [25].

On the other hand, zirconia is a polymorphic ceramic material as it changes its structure at different temperatures such as tetragonal, monoclinic, and cubic. The monoclinic structure exists between ambient temperatures to 1170 ℃. Zirconia changes into tetragonal structure between 1170 and 2370 ℃ and cubic form at temperatures between 2370 and 2716 ℃ [26,27]. Several oxide ceramics can be added to zirconia, aiming to stabilise the microstructure [28]. The addition of MgO, CaO, and Y_2O_3 to zirconia forms stabilised zirconia, which has excellent electromechanical characteristics. For example, doping zirconia with yttria (Y_2O_3) will replace Zr^{4+} with Y^{3+}, add oxygen vacancies and also increase the ionic conductivity [29]. As a result, YSZ is a popular electrolyte ceramic, which is used in solid oxide fuel cell applications. YSZ has high corrosion resistance and low thermal conductivities, which facilitate its use in micro-engine fabrication [30–32]. Besides, YSZ ceramic was successfully used to fabricate a micro-scale thruster with good shape retention and sintered shrinkage of up to 15% [33].

Silicon carbide (SiC) has become a key material for harsh environment MEMS applications. Currently, SiC wafers have been made available for MEMS fabrication. SiC ceramic has low density and high elastic modulus. This made it a popular material in high frequency MEMS resonators which are particularly important in oscillators, high sensitivity sensors, and communication transceivers [34]. Borosilicate glass is a popular material in MEMS and has been widely used in glass wafers. This is attributed to the low coefficient of thermal expansion of borosilicate glass. The low cost and the use of simple and inexpensive fabrication processes is another reason for using this material as a substrate for gas micro-sensors [35].

Polymer-derived ceramics are relatively new inorganic polymers that can be transformed into ceramic materials through thermal decomposition (pyrolysis) or oxidation process at high temperature. The unique properties of polymer-derived ceramics allow an easy shaping process by casting the material in micro-moulds. This is followed by solidification and crosslinking to form a solid polymer. Afterwards, the solid polymer is heated at 1000 ℃ to be transformed into a solid ceramic material which is capable of withstanding temperatures above 1500 ℃. Polymer-derived ceramics were also used as a binder in an alumina matrix to produce ceramic nanocomposite micro-components [36]. The electrical characteristics of polymer-derived ceramics can be controlled to be used in electrical micro-actuators and efficient micro-heaters. The outstanding thermal and chemical resistance along with the adequate mechanical properties in the harsh environment of polymer-derived ceramics makes it impossible to fabricate MEMS devices such as photonic crystals, micro grippers, and microfluidic components [37]. Micro-fabrication technologies have the ability to produce a minimum feature size of one micron from polymer-derived ceramics [37]. Recently, sub-micrometer dense and crack-free ceramic parts were fabricated using additive manufacturing of polymer-derived ceramics [21,38]. The flexibility of polymer-derived ceramics allowed the fabrication of centimetre scale parts with micro features by combining digital light processing with two-photon lithography techniques [39].

Piezoelectric MEMS uses piezoelectricity to produce motion and carry out a specific task. It develops a potential difference between two of its faces when its thickness changes (sensor) and physically changes its shape when electricity is applied (actuator). Lead zirconate titanate (PZT) is one of the most used piezoelectric materials. It can be used as both sensors and actuators in applications such as micro- pumps, energy harvesters, inkjet printer heads, and RF MEMS [40]. A summary of ceramic materials used in MEMS is shown in Table 1.

3 Micro-fabrication technologies

Micro-fabrication technologies of ceramic materials can be grouped into three categories, as shown in Fig. 3:

Table 1 Comparison of ceramic MEMS materials

Material	Processing	Applications	References
LTCC	Lithography, electro-phoretic deposition, aerosol jet printing, laser micro machining	Substrates, micro-electronics, micro-fluidics, sensors, packaging	[41–47]
Alumina	Soft lithography, etching, micro-injection, electro-phoretic deposition, extrusion, μEDM	Nano/microelectronics, magnetic storages, photonics, micro-engines	[48–55]
Zirconia	Soft lithography, etching, micro-injection, electro-phoretic deposition, extrusion	Photo electronics, micro-engines, sensors, nano-arrays, micro-tubes	[56–60]
Silicon carbide	Soft lithography, etching, micro-injection, extrusion, μEDM	Photonics, diodes, thin-film transistors, sensors, combustion, micro-actuators	[61]
Borosilicate glass	Lithography, micro machining, hot embossing, μEDM	Substrates, sensors, grippers, micro-fluidics, micro-mirrors, packaging	[62–67]
Polymer-derived ceramics	Lithography (soft, nanoimprinting, nano stereo)	Actuators, photonics, electrical heating, micro-fluidics	[68]
Lead zirconate titanate	Lithography, etching, micro-injection, electro-phoretic deposition, extrusion	Sensors, actuators (micro-pumps, energy harvesters), RF MEMS	[69–73]

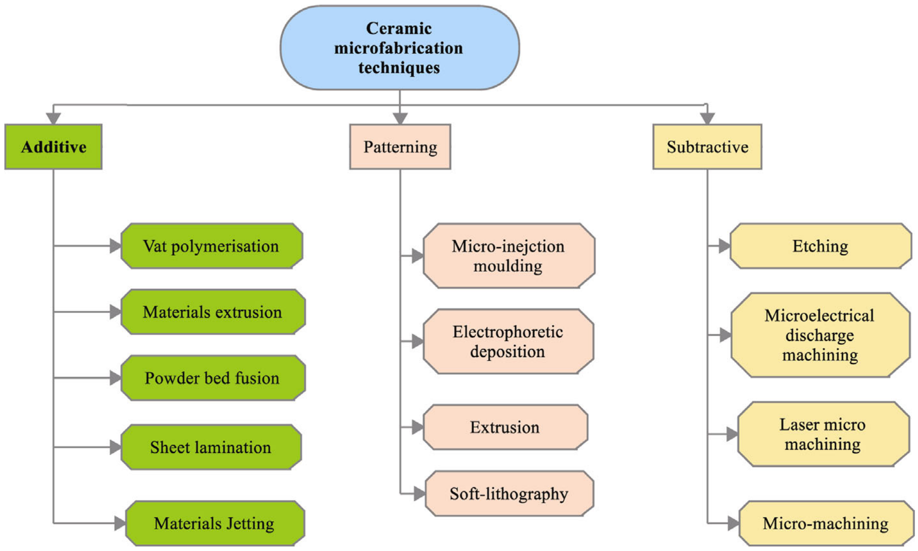

Fig. 3 Micro-fabrication technologies of ceramic materials.

(1) additive manufacturing (AM), (2) patterning, and (3) subtractive techniques. AM techniques include fused deposition modelling (FDM), stereolithography (SLA), laser micro sintering (LMS), sheet lamination (SL), and materials jetting (MJ). Conventional micro-fabrication techniques are based on silicon micro-lithographic processes such as patterning and subtracting [74]. Patterning techniques include micro-injection moulding (μIM), electro-phoretic deposition (EPD), extrusion, and soft-lithography (SL). Furthermore, subtractive techniques include etching, laser micro-machining (LMM), micro-electrical discharge machining (μEDM), and micro-machining.

3.1 Additive techniques

Additive manufacturing (AM) is an emerging group of manufacturing technologies that have been developing over the past three decades. Stereolithography apparatus (SLA) is the first AM technology which was invented by Charles Hull in 1986 to create 3D objects using ultraviolet light (UV) to cure polymer layers incrementally. Since then, several AM techniques have been developed, and a wide range of applications have been enumerated [75–80]. The following sections discuss each of AM techniques used in MEMS fabrication.

3.1.1 Vat polymerisation

Vat polymerisation (VP) is a technique that uses UV to repeatedly cure layers of photosensitive polymer until the build is completed, as shown in Fig. 4. The completed object is then detached from the building

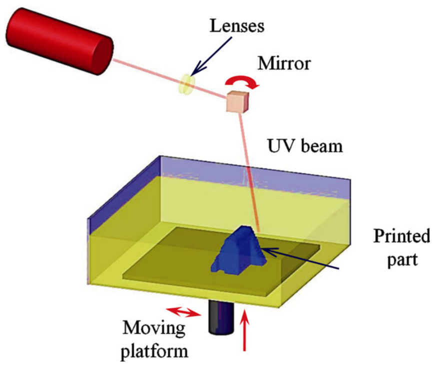

Fig. 4 A schematic diagram of VP process.

platform, and post-processing may be carried out, such as cleaning or heating, to obtain improved structural integrity and mechanical properties. Printed parts developed using this technique typically have high resolution and accuracy. However, the building rate of this technique is relatively slow and restricted to photosensitive resins. VP of ceramic micro-fabrication is developed by using either direct or indirect approaches. In direct manufacturing, ceramic particles are dispersed in a photosensitive resin to achieve the required properties such as solid loading and viscosity. Throughout the printing process, the ceramic mixture is deposited until the green parts are completed and then used in a VP 3D printer to achieve the green micro parts. This is followed by a de-binding process to remove polymer additives. Finally, the free parts of the polymer are sintered using a sintering furnace.

On the other hand, indirect manufacturing includes the use of micro moulds (permanent or lost) that are fabricated using the VP of a polymer. The ceramic suspension is usually prepared by mixing up the ceramic powder with dispersant, water, and a binding agent. Next, the prepared ceramic slurry is poured into a 3D printed mould and left to cure and dry. Afterwards, cured parts are demoulded from the printed mould. Similar to the direct method, the cured parts are de-bounded and sintered in a kiln to obtain the final micro parts [81]. Stereolithography (SLA), continuous liquid interface production (CLIP), two-photon polymerisation, and digital light processing (DLP) are techniques that have been developed within the VP family. In micro stereolithography, UV beam is focused on a focal point of a vat filled with photosensitive resin, which initiates the photopolymerisation. The laser is controlled using a computer numeric control (CNC) whereas a shutter is used on and off to ensure that the photopolymerisation is achieved. Complex-shaped ceramic parts with high accuracy were successfully fabricated using SLA of different ceramic materials [82]. De Hazan and Penner [83] used SLA process to fabricate complex-shaped parts using allylhydridopolycarbosilane (AHPCS) and multifunctional acrylates. He *et al.* [84] fabricated 3D printed ceramic structures using SLA combined with precursor infiltration and pyrolysis. Firstly, micron-sized SiC powder-based slurry was prepared and used in SLA process. The resin material was de-binded, and porous SiC parts were achieved. An infiltration with polymer derived ceramics followed by pyrolysis was used to improve the density. Two- photon polymerisation scanning micro stereolithography is to fabricate higher resolution features down to the nano-size. In this process, a resin molecule absorbs two photons from top and bottom, creating simultaneously higher energy, which can be realised by using a femtosecond laser. Digital light processing (DLP) uses dynamic photomask. The process uses UV illumination to cure an entire layer which can control the intensity of every pixel, and hence the resolution of the 3D printed features. Wang *et al.* [85] introduced a rapid thiol-ene chemical reaction based polymer derived ceramics for the use in both SLA and DLP processes. Through photo cross-linking, polymer derived ceramics transform into cured micro-parts. This is followed by a pyrolysis process to transform the printed parts into amorphous ceramics with nearly fully dense, porous, and defect-free and high-quality surface finish.

Liu *et al.* [86] developed a micro-stereolithography approach to fabricate alumina and zirconia micro-components with high density and controlled grain size. The authors mixed the ceramic powder with photosensitive polymers using powder milling and ultra-sonication to prepare homogenised powder mix suitable for a stereolithography 3D printer. Figure 5 shows several manufactured microcomponents, including periodic arrays, micro gears, microcellular, and microturbines, with no visible defects. Similar research has been carried out to prepare alumina [87,88], barium titanate [89], polymer derived ceramics, and alkaline niobate-based lead-free piezoceramics using micro-stereolithography ceramic suspension [90].

On the other hand, polymer derived ceramics were employed for a stereolithography process. Complex-shaped micro-cellular structures were fabricated using polymer derived ceramics mixed with a photoinitiator. Then, the printed polymer structures were pyrolysed to develop a high-temperature resistance silicon oxycarbide ceramics with uniform shrinkage and no visible porosity (see Fig. 6). The mechanical strength of developed AM honeycomb cellular structure outperformed the conventionally made ceramic foam.

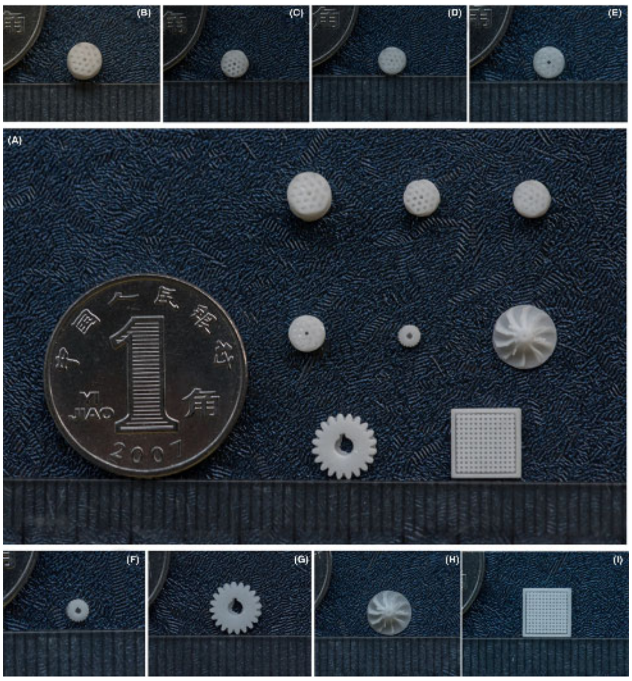

Fig. 5 Alumina and zirconia ceramic micro-components fabricated using stereo-lithography: (B–E) cellular structures with different pore size and helical structure, (F, G) different size micro-gears, (H) turbine micro-rotor, (I) columnar array with pillar diameter of 100–200 μm. Reproduced with permission from Ref. [86], © The American Ceramic Society 2018.

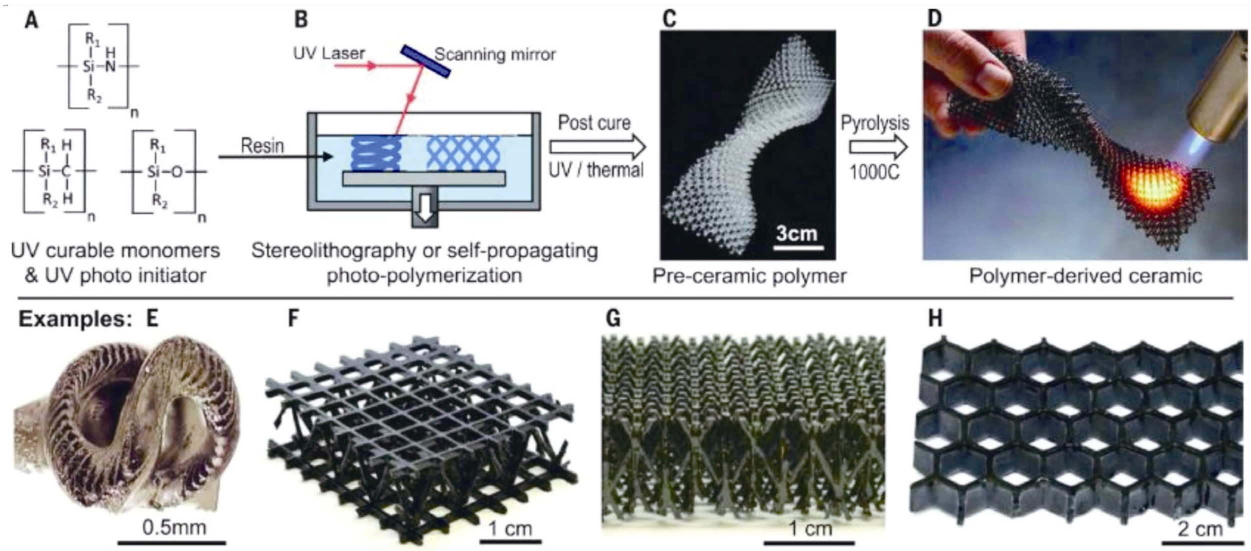

Fig. 6 (A) Mixing of UV-curable preceramic monomers with a photoinitiator. (B) 3D printing process of the mixed polymer. (C) Printed micro-lattice. (D) Pyrolysis into ceramic material. (E–H) Several cellular examples. Reproduced with permission from Ref. [91], © American Association for the Advancement of Science 2016.

Digital light processing (DLP) was also implemented to fabricate ceramic micro-parts. Most of the research on using DLP for ceramic micro-fabrication is based on the use of polymer-derived ceramics as a monolithic polymer or mixed with ceramic fillers. The photosensitive resin was prepared using polymer-derived ceramics and a photoinitiator. Silicon nitride, SiOC, and mullite green ceramic micro-lattice structures were first printed using a DLP 3D printer. Afterwards, the green parts are placed in 1400 ℃ furnace with nitrogen in a pyrolysis process. Figures 7 and 8 show SEM micrographs of micro-lattices with the complex structure before and after sintering. The printed cells had no rounded edges. In addition, the stair-stepping can be seen in the developed structure. Furthermore, no delamination or cracking can be noticed in the printed layers [92–95]. Initial trials on using MicroCLIP process were carried out to fabricate hydroxyapatite (HA) based scaffold with micro-cellular feature, though no de-binding or sintering processes were carried out [96].

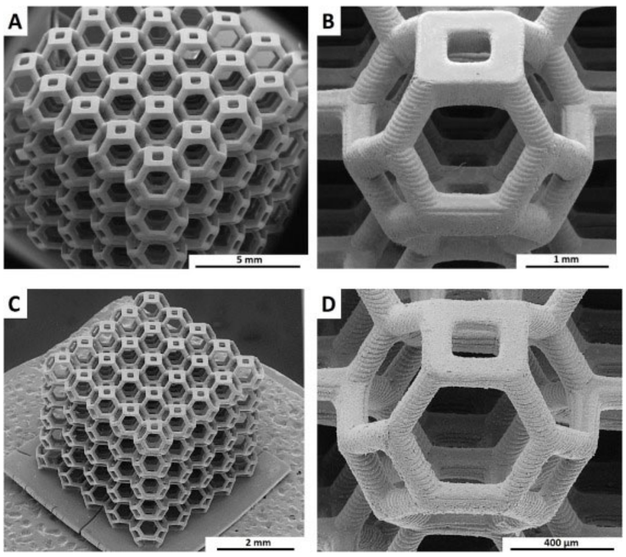

Fig. 7 SEM micro-graphs of (A, B) dried and (C, D) pyrolysed samples. Reproduced with permission from Ref. [93], © Elsevier Ltd. 2017.

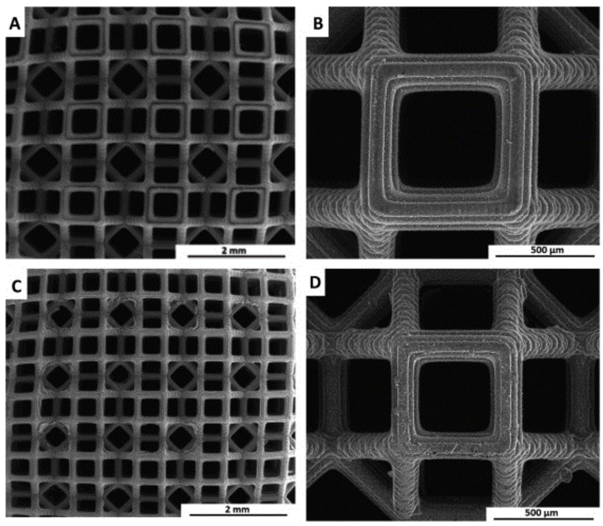

Fig. 8 SEM images of micro-cellular structure 3D printed using polysiloxane/alumina composite: (A, B) as printed, (C, D) after sintering. Reproduced with permission from Ref. [94], © Elsevier Ltd. 2018.

3.1.2 Material extrusion

Material extrusion (ME) is a simple, available, and affordable additive manufacturing technique [78,97,98]. In ME, a paste or thermoplastic filament is extruded through a small nozzle following a controlled track of a slice of a digital model. Figure 9 shows a schematic diagram of material extrusion. Thermoplastic materials are typically used in FDM ME technology such as poly-lactic acid (PLA), high-impact polystyrene (HIPS), and polyurethane (TPU). In addition, pastes and gels are printed using a pneumatic pressure (PE) or a syringe (SE). The fabrication process of PE/SE starts with extruding the material through a small nozzle using the PE or SE. The quality of ME printed objects is affected by several parameters including material, printing speed, layer thickness, geometry, nozzle diameter, nozzle, and building platform temperatures.

SE of HA/TCP ceramic suspension to manufacture scaffolds with micro-pores and controlled morphologies were introduced [99]. The developed pore size of the sintered scaffolds was found to be about 200 μm. Robocasting (RC) or direct ink writing is a syringe extrusion method that is based on the extrusion of ceramic suspension. The technique starts with the deposition of highly concentrated colloidal ceramic suspension with a concentration in a range of 35–50 vol%. An optimised ceramic ink with appropriate rheological and viscoelastic properties must go through a fine nozzle and should have the ability to support its weight during printing. The printed parts typically have excellent shape retention and adequate mechanical properties. Robocasting was invented by Sandia National Laboratories as free-forming objects and has been developed further to fabricate ceramic MEMS. Robocasting is considered as one of the most available and reliable techniques to fabricate very fine, near-net shape, and dense ceramic structures with complex geometries. Cai *et al.* [100] prepared a concentrated SiC ceramic ink with a concentration of 44 vol% and Al_2O_3 and Y_2O_3 as sintering additives for the deposition of complex-shaped structures. Colloidal powder processing route was successfully implemented by controlling the addition of different dispersants for controlled dispersion and flocculation. Various inks were prepared with different strength, and the strong ink was found optimum for robocasting. Lattice structures with a strut thickness of 200 μm were deposited, dried, and sintered using spark plasma sintering at 1700 ℃. The sintered lattice structures were transformed from β-SiC to α-SiC and reached a density of 97%. The fabrication of biomedical scaffolds with micron-size channels and struts were successfully developed using robocasting. Touri *et al.* [101] developed biomedical scaffolds using hydroxyapatite (HA) and beta-tricalcium phosphate (β-TCP) powder mixture. The robocasting process was used to fabricate porous 3D lattice structures. In addition, calcium peroxide, which is an antimicrobial material, was mixed with a polycaprolactone (PCL) solution to prepare an antimicrobial coating. The printed and coated scaffold demonstrated an adequate porosity level with a minimum feature size of 400 μm, an antibacterial coating, and improved alkaline phosphatase activity, which makes robocasting a promising tool to manufacture bone scaffolds. Figure 10 shows the optical and SEM micrographs of the sintered robocast scaffolds. The porosity was found 70% with an average open pore size of 300–500 μm, which are typical values for bone formation both *in vivo* and *in vitro*.

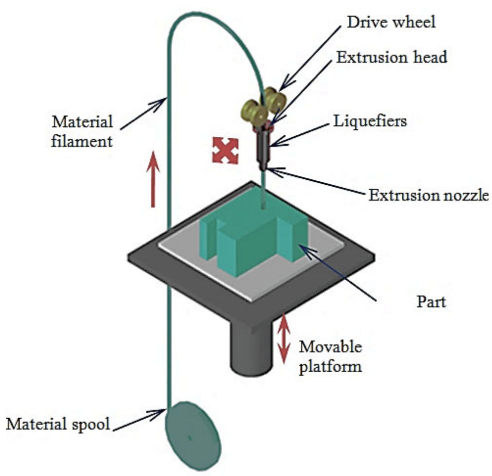

Fig. 9 Schematic illustration of FDM technique.

Research on the manufacturing of ceramic micro parts using FDM technologies is lacking. This is attributed to the poor resolution, poor surface roughness, and interlayer defects of the process compared to techniques such as stereolithography. On the other hand, as FDM is based on extruding thermoplastic filament to achieve printed parts according to digital design. Therefore, it was expected that the technique would be able to process filament made of polymer-derived ceramics. However, no published research has been yet introduced in this direction. This is maybe because solid form filaments made of polymer-derived ceramics are rigid and cannot be made into as spool [102].

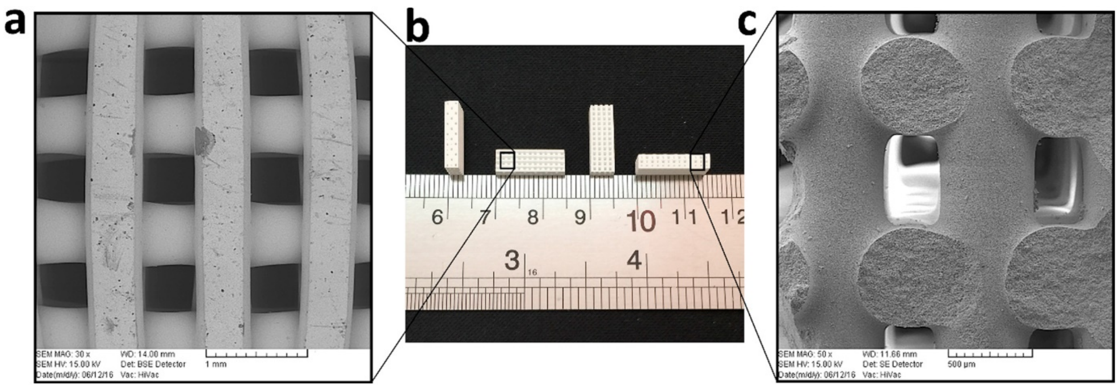

Fig. 10 Sintered printed HA/β-TCP scaffold: (a, c) SEM micro-graphs of the top view and (b) cross section optical image of the ceramic scaffold. Reproduced with permission from Ref. [101], © Elsevier Ltd and Techna Group S.r.l. 2018.

3.1.3 Powder bed fusion

In powder bed fusion (PBF), heat energy is applied through a source such as an electron or laser beam to sinter or melt a layer of the powder according to a specific digital model layer by layer. The laser or electron bean selectively scans and fuses a layer of powder. The building platform incrementally drops down, and another layer is spread on the top surface of the preceding one. The steps are repeated until the part is built. This approach becomes a popular technique in aerospace, healthcare, defence, and automotive industries. Selective laser melting (SLM) and electron beam melting (EBM) have the ability to melt metal alloy in full density and adequate mechanical properties [103]. Meanwhile, selective-heat-sintering (SHS) and selective laser sintering (SLS) can only increase the temperature of the processed powder below the melting point [104–108] (see Fig. 11).

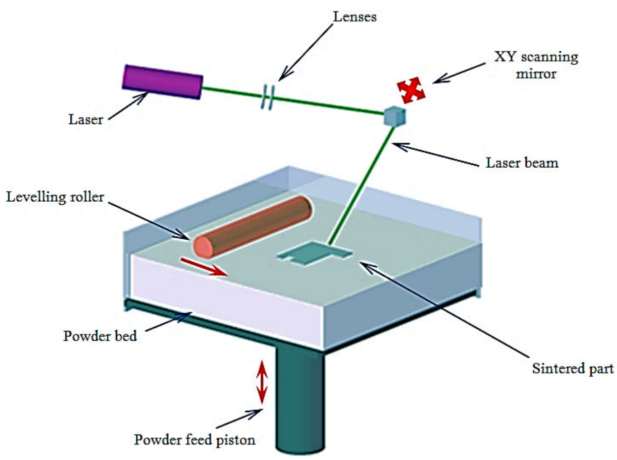

Fig. 11 Schematic diagram showing the powder bed fusion approach.

Experimental work on the use of SLS of ceramics micro-components was focused on printing, de-binding, sintering, and infiltrating them to enhance their density. Typical SLS/SLM machines are able to create micro-features of about 100 μm. The process was modified by Laser Institut Mittelsachsen to achieve micro parts with an aspect ratio greater than 10 and improve the resolution of the part to about 50 μm and a roughness (*Ra*) of 1.5 μm by using (Nd:YAG) laser. Additionally, the use of CO_2-laser was found to be inappropriate in laser processing of ceramics due to laser diffraction for wavelengths near IR and VIS [109]. The developed system uses a raking process to create a thinner powder layer with a submicron particle size to fabricate ceramic micro-components with excellent resolution. However, the archived density is less than those in bulk materials. Petsch *et al.* [110] studied the use of micro SLS technique to manufacture microcomponents made from metal and ceramic powders for miniaturised tools and products. The process has successfully fabricated micro-parts for tools from ceramic powders such as aluminium nitride. Other ceramic materials, including alumina, SiO_x, and SiC or SiSiC have been developed using laser micro sintering [111,112]. Laser micro sintering approaches of ceramic micro parts has become less favourable and the publications found in this area are quite few. On the other hand, bulk powder bed fusion systems have been increasingly implemented to produce ceramic micro components but with lower resolution than LMS. Essa *et al.* [113] introduced a novel approach to developing an alumina micro-cellular structure for monolithic catalyst bed applications. The authors used a typical SLM machine to produce aluminium precursor micro-cellular structure with strut size of 150 μm followed by a heat treatment to achieve alumina structures. The developed catalyst bed was found to outperform the conventional ceria pellet-based catalyst bed, as shown in Fig. 12.

3.1.4 Sheet lamination

Sheet lamination (SL) glues layers of sheets and cuts them using a cutter or a laser beam. Ultra-sonication may be applied locally to enhance the bonding quality of the stacked sheets. Post-processing steps such as machining and surface finishing may be used after the completion of the build. The bonded layers are stacked layer-wise to build the physical part (see Fig. 13). SL can process plastic, ceramic, paper, or metal laminates. This technique is partly subtractive as it cuts the contour of the sheet laminate. Additionally, SL is one of the rapid AM approaches to print complex geometries. Nevertheless, it is challenging to control interlayer defects. SL is not a typical approach to fabricate ceramic micro components. However, a study introduced by Windsheimer *et al.* [114] studied the SL technique to manufacture ceramic Si–SiC micro parts using SiC-loaded preceramic polymer sheets. The prepared sheets were covered with an adhesive to glue them together before SL process. Following printing, a pyrolysis process was carried out by placing the green parts in a furnace under N_2 environment at 800 ℃ followed by infiltration with Si at 1500 ℃ under vacuum conditions. This leads to micro-ceramic components with a laminar microstructure of Si–SiC as shown in Fig. 14. The properties of the developed objects were found dependent on the direction of the layers with respect to loading.

3.1.5 Material jetting

Material jetting (MJ) jets droplets of a material using a print head to make a 3D object or a thin film then dried or get cured under UV exposure, as shown in Fig. 15. MJ was first invented by Objet Ltd. and then merged with Stratasys to combine the photopolymers and Inkjet technologies. MJ technology can print objects in

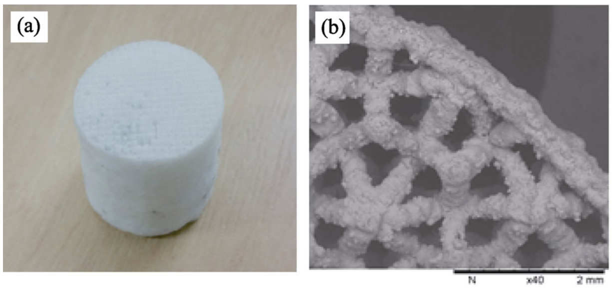

Fig. 12 Catalyst bed cellular structure: (a) optical image, (b) magnified SEM image. Reproduced with permission from Ref. [113], © Elsevier B.V. 2017.

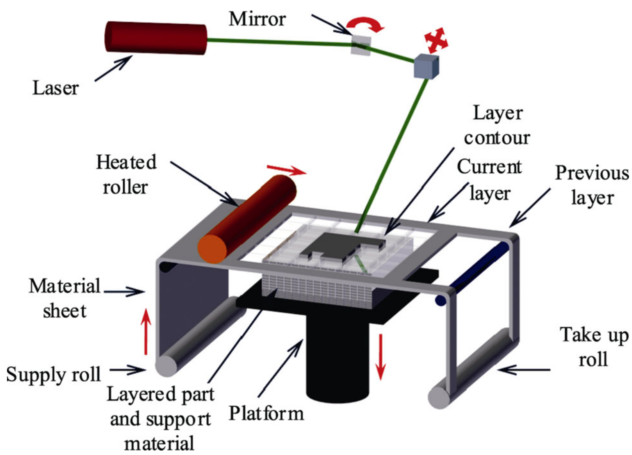

Fig. 13 Sheet lamination process.

full colours and high-quality finishing. MJ is capable of processing polymers and waxes through the deposition of droplets through a nozzle. The use of wax as support material provides an excellent surface finish to the printed objects. MJ processes various polymers such as polymethyl methacrylate (PMMA), high-density polyethene (HDPE), polycarbonate (PC), polystyrene (PS), and polypropylene (PP). In addition, polymer materials loaded with ceramic particles were also processed using MJ [115]. In drop on demand (DOD) the material is deposited only when required using a discrete pressure. Additionally, continuous inkjet deposits the material through a nozzle using a continuous pressure [116]. To prepare a ceramic slurry,

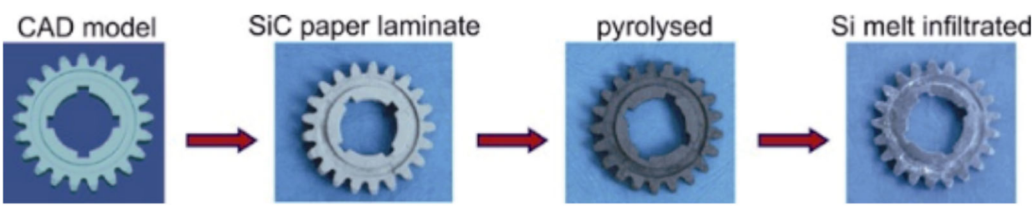

Fig. 14 SL fabrication process of Si–SiC micro gears. Reproduced with permission from Ref. [114], © WILEY-VCH Verlag GmbH & Co. KGaA 2007.

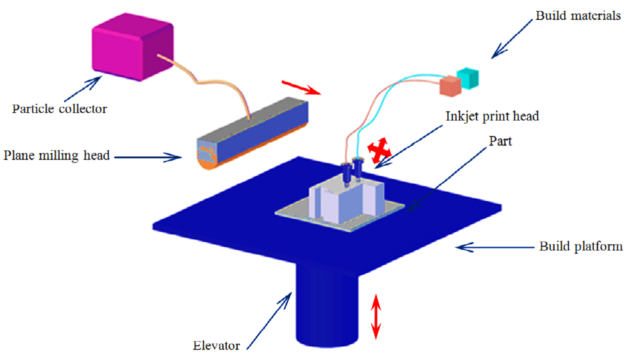

Fig. 15 Schematic diagram of the material jetting process.

ceramic powders, binders, and dispersants are mixed and placed in the 3D printer head. Rheological characteristics of ceramic suspension play an important role to obtain homogenous and dense green parts. Ainsley *et al.* investigated the use of inkjet 3D printing of ceramic suspensions to print 3D structures by controlling ceramic droplet deposition. Alumina was suspended in an alkaline suspension [117]. Free-standing parts such as rotating wheels and structures with a thickness of 100 μm were demonstrated. Similarly, zirconia ceramic micro walls were also developed by Zhao *et al.* [118]. The authors developed sintered ceramic micro maze with a wall thickness of about 170 μm as depicted in Fig. 16.

Table 2 shows a summary of the current AM capabilities to fabricate ceramic MEMS and lists their best resolution, processed materials, and examples of applications.

Fig. 16 SEM image of the sintered maze built by ink-jet printing. Reproduced with permission from Ref. [118], © The American Ceramic Society 2002.

Table 2 Summary of AM techniques used for MEMS fabrication

Technique	Physical form	Shaping	Resolution	Materials	Examples	References
Micro stereo lithography	Powder-resin mixture	UV curing, de-binding, sintering	150 nm	Alumina, barium titanate, alkaline niobate, polymer derived ceramics, zirconia	Micro lattices, micro rotors, micro gears, micro turbines, Arrays	[81,86–91]
Digital light processing (DLP)	Powder-resin mixture	UV curing, de-binding, sintering	100 μm	Polymer derived ceramics, alumina, silicon nitride, SiOC, and mullite	Micro-lattices, micro-mirrors	[92–95]
Continuous liquid interface production (CLIP)	Powder-resin mixture	UV curing, de-binding, sintering	64 μm	Polymer derived ceramics	Micro-lattices, micro-rods	[96]
Robocasting	Suspension	Deposition, drying, de-binding, sintering	76 μm	SiO_2, Al_2O_3, mullite, HA, TCP, bioglass, Y_2O_3/ZrO_2, SiC, Si_3N_4, B_4C, ZnO, $BaTiO_3$	Micro-lattices, scaffolds, micro-channels	[22]
Fused deposition modelling (FDM)	Filament followed by de-binding and sintering	Extrusion, de-binding, sintering	200 μm	Tricalcium phosphate/hydroxyapatite	Scaffolds with micro sizes pores	[99]
Laser micro sintering (LMS)	Powder	Laser beam consolidation	50 μm	Alumina, SiO_x, and SiC or SiSiC, aluminium nitride	Catalyst bed with micro lattices, micro springs, free-standing walls, microturbines	[109–113]
Sheet lamination (SL)	Tape shaped, followed by de-binding and sintering	Cut, glue, de-binding, sintering	—	Si–SiC	Micro gears	[114]
Ink-jet printing	Ceramic powder shaped, followed by de-binding and sintering	Binder jetting, drying, de-binding, sintering	100 μm	Alumina, zirconia	Micro maze	[118]

3.2 Patterning

3.2.1 Micro-injection moulding

Micro-injection moulding (μIM) of ceramics works in a very similar way to the conventional bulk plastic injection moulding. It is used to manufacture different sizes, shapes, and materials. The process starts with preparing the feedstock by mixing low melting temperature polymer or wax with metal or ceramic powder to be injected into the cavity of a die with micro-cavity, as shown in Fig. 17. The die is left to cool down to allow the shaped micro parts to be ejected. The ejection step can be problematic, especially for parts with high aspect ratio and small feature size. This technique can work at a temperature and a pressure of 60–100 ℃ and 2 bar, respectively, which suits the use of soft and photo-resist moulds. The green objects are then de-bound and sintered. The slow thermal de-binding process is typically carried out at a heating rate as small as 0.1 ℃/min [119–122].

Over the past three decades, much research has been carried out on ceramic micro-injection moulding. This includes material variation, mould design and manufacturing and process controlling. In this technique, the feedstock is made by mixing ceramic powder and thermoplastic polymer or a binder to be injected under high pressure and temperature to fill the micro-cavities of the die. It is crucial to select the appropriate powder morphology and size together with an appropriate binder to meet the requirement of feedstock properties. The irregularity of ceramic powder generates high green strength samples due to the particles' plastic deformation [123,124]. On the other hand, the spherical powder is typically used in the preparation of the feedstock. Binder removal can be achieved by either thermal de-binding or solvent leaching. Micro-injection moulding has the advantages of creating complex shapes in mass production. Typical defects of injection moulding include the inhomogeneous density, flow lines, warping, air pockets, sink marks, weld lines, delamination, and flash [125,126]. Ceramic materials used in micro-injection moulding include zirconia, alumina, silicon nitride, and silicon carbide [52,127]. Figure 18 shows the micrographs of zirconia microcomponents fabricated by using microinjection moulding.

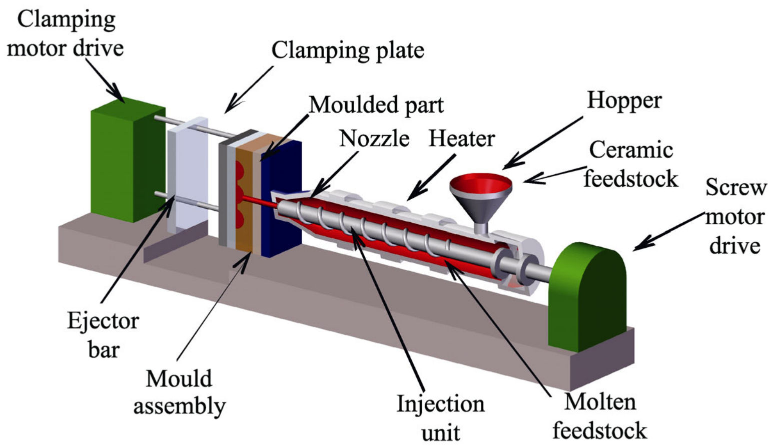

Fig. 17 Schematic diagram of the micro-injection moulding process.

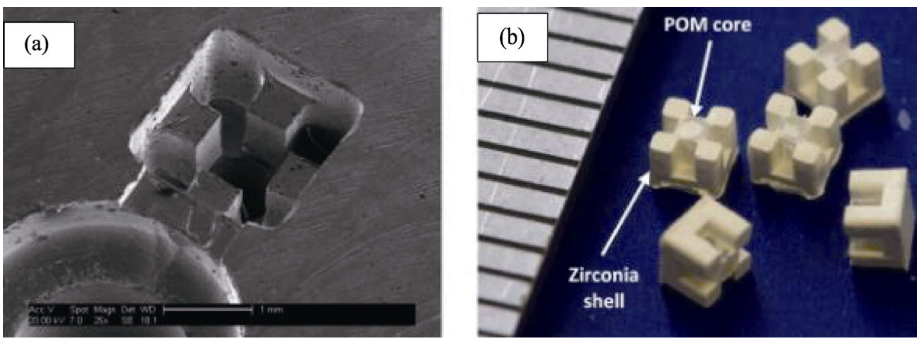

Fig. 18 (a) SEM micrographs of a micromould insert. (b) Replicated zirconia micro components. Reproduced with permission from Ref. [128], © Elsevier Ltd. 2012.

3.2.2 Electro-phoretic deposition

In electro-phoretic deposition (EPD), an electric current is applied to a highly dispersed so that the suspended particles charge, flow and deposit on the surface of an electrode, as shown in Fig. 19. In EPD, colloidal particles such as polymers, ceramics, and metals carry a surface charge and thus can be attracted to the opposite change electrode [129–133]. Green parts can be demoulded and sintered once the particles fill the mould cavity. As a result, electro-phoretic deposition allows the deposition of ceramic films on patterned and non-flat moulds [12]. Mould surface must be conductive or coated with a conductive later before they are used in this process. A drawback of electro-phoretic deposition is the achieved low density of the developed parts (see Fig. 20). Zaman *et al.* [134] deposited alumina–CNT thin films onto micro pattern moulds prepared using 3D printing. Firstly, micro gears were designed using CAD and created using a 3D printer. The moulds were glued on top of a conductive metal substrate. The EPD suspension was prepared by using aluminium acetate powders and CNT aiming to produce CNT-reinforced alumina nano-powders. Afterwards, EPD was used to achieve near net green micro-gears and was followed by sintering.

3.2.3 Extrusion

Extrusion is an approach to produce micro parts of uniform geometries such as rectangular, honeycombs, and cylinders. The technique could be used to shape several materials. Extrusion is similar to injection moulding; the molten thermoplastic mixture is extruded through a nozzle with a uniform cross-section, as shown in Fig. 21. The difference between the two techniques is in the form of the dies [135]. There are several types of extrusion methods such as screw extrusion, ram extrusion, co-extrusion, hollow fibre extrusion, and single-layer extrusion; however, co-extrusion is the most widely used technique used for micro-fabrication. Both extrusion and injection moulding dies are relatively expensive and have a short lifetime due to the high friction between ceramic paste and the die. The choice of the die shape plays a key role in the wear rate. Simple geometries and thicker components require low pressure which reduces the abrasion. Therefore, extruding a solid rod is more efficient than extruding a hollow one. Size reduction is achieved when patterning micro parts using the extrusion process. After extruding the green parts, a typical de-binding and sintering process takes place [136]. The viscosity of the prepared paste and the applied pressure have a great effect on the characteristics of the

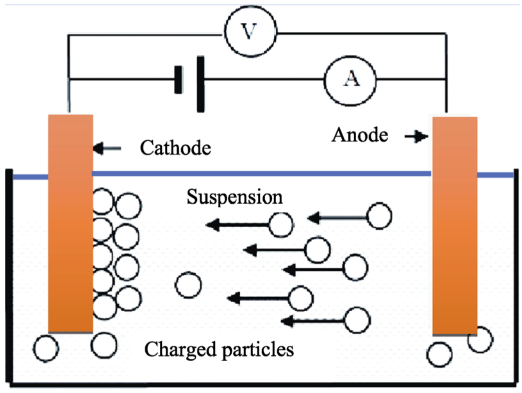

Fig. 19 Schematic diagram of electro-phoretic deposition and electroforming principal.

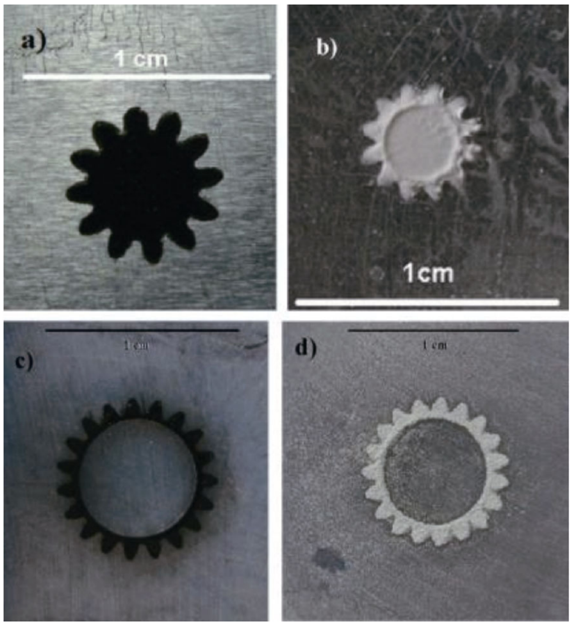

Fig. 20 (a) Micro mould, (b, d) micro-gears before sintering, (c) EPD 1 wt% CNT-reinforced alumina. Reproduced with permission from Ref. [134], © Elsevier Ltd. 2010.

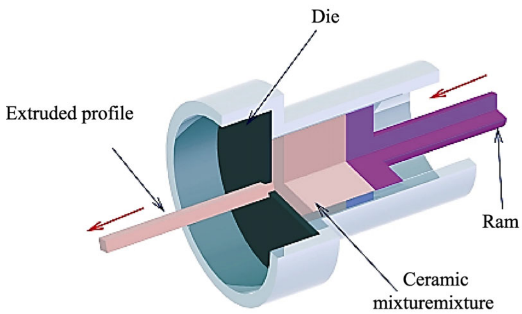

Fig. 21 Schematic diagram of the extrusion process.

green parts and hence the quality of the components. However, de-binding and sintering are two critical processes that require much attention. Thermal binder removal is an important stage as the entrapped gas pressure can increase due to the uncontrolled binder decomposition and possibly produce cracks and defects [137]. These considerations also apply to the micro-injection process as well. The process shows success in producing bifunctionally graded materials. Sharmin and Schoegl [138] investigated the use of co-extrusion to develop multi-layered, functionally graded, and/or textured mesoscale combustors. To prepare the feedstock, alumina powder, polyethylene glycol (PEG), and polyethylene butyl-acrylate (PEBA) were mixed in a rheometer. Next, the feedstock was extruded through 5.84 mm die. The authors used solvent and thermal debinding to remove the binders' contents before sintering at 1600 ℃. Other applications include microtubes for solid fuel cells [139], piezoelectric actuators [140], and combustors [138]. Microrods were also prepared by co-extrusion of zirconia–alumina bi-layer. Microrods with various thicknesses were fabricated using co-extrusion. Figure 22 shows SEM images of sections of the fabricated bi-layers with various thicknesses [135]. A feature size of 10 μm was successfully achieved using co-extrusion [141].

3.2.4 *Soft-lithography*

Soft-lithography (SL) is a non-photo-lithographic process which is based on replica moulding. The technique is well established to fabricate ceramic, metal, and polymer replicas [142]. In the soft lithography, a soft mould is implemented with patterned relief micro features to generate micro and nano components. Materials used to prepare soft moulds to include poly-dimethylsiloxane (PDMS) elastomers, polyurethanes, polyimides, and Novolac resins. The technique is popular because it is relatively cheap and produces parts with high accuracy. There are five types of soft lithography, and they are micro-moulding in capillaries, micro-transfer moulding, micro-contact printing, replica moulding, and solvent assisted micro-moulding [143–146]. Typical stages of SL technique are: creating the soft mould, preparing the metal and ceramic slurries (a mixture of binder and powder), filling up the soft mould with the prepared slurry, drying/curing and demoulding, de-binding and sintering to achieve the consolidated micro parts. Soft moulds are typically produced using photo-resist master mould representing the negative replica of the soft mould [147–157]. Hassanin and Jiang [158] developed a process to replicate soft mould micro/nano-patterns using another soft mould rather than using the typical photoresist-based solid mould with the aid of surfactants or a gold layer as release agents. Micro-contact printing (μCP) is one of the soft lithography techniques that uses an elastomer mould as a stamp to form micro-patterns of ink or a suspension onto a surface of a substrate via conformal contact, as shown in Fig. 23(a). The process is similar to the typical stamping to transfer ink from a pad to a paper. It is a flexible process since it is possible to use the planar or rolling stamp on a planar surface. It is simple, inexpensive, and very efficient [159–161]. Micro-transfer moulding (μTM) on the other hand uses a soft patterned mould in which a drop of a liquid pre-polymer such as a ceramic slurry is used to fill up the cavities of the soft mould. The excess suspension can be cleared using a flat razor blade. Next, the micro-mould is left to cure or dry. Afterwards, the parts are gently peeled away to achieve the micro-parts on the top of the substrate, as demonstrated in Fig. 23(b). In this process, complex-shaped and free-standing micro-components can be processed. One of the most significant advantages of μTM is its potential to fabricate micro patterns on non-planar surfaces [162–164]. In micro-moulding in capillaries (MIMIC), soft mould is placed face down on a substrate aiming to achieve a conformal contact. Next, a low-viscosity suspension is dropped at the side opening of the microcavities, which allows it to fill the microcavities by using capillary action. The mould is left to dry and peeled off to achieve a micro pattern on top of the substrate (see Fig. 23(c)). The process also can form micropatterns for flat and non-planner surfaces. Additionally, MIMIC can be implemented to pattern other materials, including ceramic precursor polymers, UV-sensitive polymers, solutions, and sol-gels [165–167].

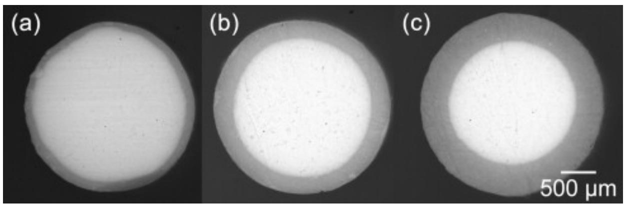

Fig. 22 SEM images of cross-sections of zirconia toughened alumina micro rods prepared using initial alumina thickness of (a) 0.5 mm, (b) 1.0 mm, (c) 1.5 mm. Reproduced with permission from Ref. [135], © Elsevier Ltd. 2015.

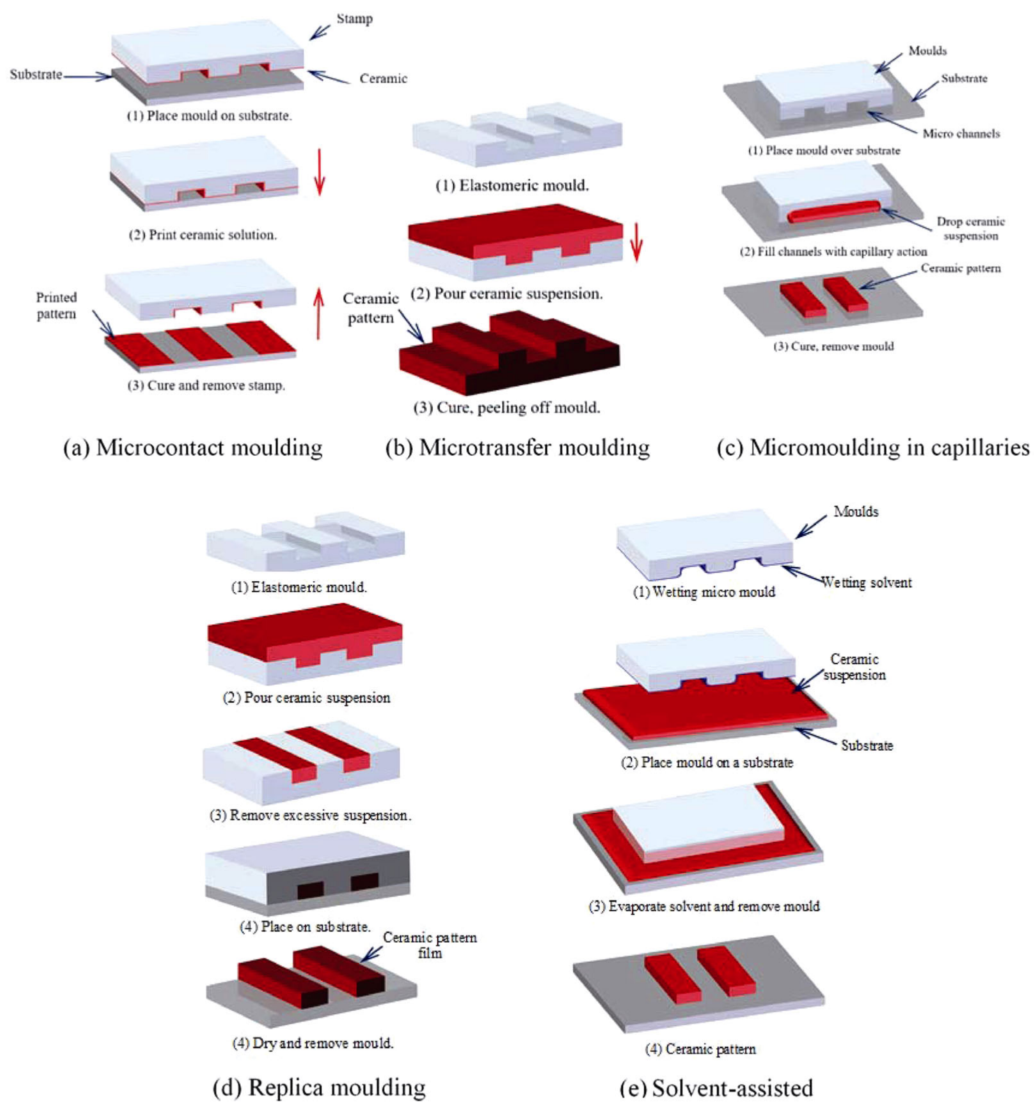

Fig. 23 Soft-lithography techniques. (a) Micro-contact moulding. (b) Micro-transfer moulding. (c) Micro-moulding in capillaries. (d) Replica moulding. (e) Solvent assisted micro-moulding.

Replica moulding is another soft lithography process that is used to replicate patterns from an elastomeric mould into another surface by liquid solidifying, as shown in Fig. 23(d). Several ceramic suspensions can be used and cured using replica moulding. The process has the ability to pattern structures in nanometers [168]. Solvent assisted micro-moulding (SAMIM) is another soft lithography process that is used to fabricate micro-components with the assistance of a solvent. In this process, the prepared suspension is applied on a plate while the mould is wetted using a solvent. Afterwards, the soft mould is placed on a layer of suspension. The solvent wets the cavities and helps to fill up the micro-cavities with the polymer. Next, the solvent is evaporated, and the suspension is cured or dried to obtain the micro-patterns (see Fig. 23(e)) [169,170].

In 1999, Schönholzer *et al.* [171,172] introduced a manufacturing process to develop alumina micro-patterns using soft-lithography. Figure 24 shows the patterned micro-holes using soft lithography. Alumina samples fabricated in this research reached a full density and a shrinkage of 15% (hole resolution: 3 μm). Hassanin and Jiang [173] studied the effect of the size of the ceramic powder on the rheological characteristics, and the quality of developed microcomponents using three powder sizes. The study evaluated the stability of the prepared suspensions when changing the dispersant amount. The properties of the dried and fired samples in terms of shrinkage, shape retention, and hardness values were also investigated. It was found that the axial shrinkage of the microparts increased by using a smaller particle size. In addition, the part shape retention, resolution, and roughness were dependent on the size of the powder. As the particle size decreased, the micro-part resolution and the surface roughness improved (see Fig. 24). The authors carried out several research projects on soft lithography to produce free-standing alumina micro components [173–177]. Table 3 shows a summary of the patterning techniques.

3. 3 Subtractive processes

3.3.1 Etching

The etching process is categorised into two groups: wet & dry etching. In wet etching, silicon oxide is etched by immersing oxidised silicon wafer into an etchant which dissolves micro features (see Fig. 25). On the other hand, the dry etching process is a physical process in which micro features are achieved by milling using a focus ion beam or using reactive ion etching [181,182]. Using this technique, identical features at one wafer and free-standing micro components with high accuracy can be fabricated [70].

As shown in Fig. 27, a typical etching process of ceramic may involve several steps and techniques such as photo-lithography, self-assembly, or micromachining. For example, Liu *et al.* [183] studied the micro-fabrication of free-standing $La_{0.7}Sr_{0.3}MnO_3$ (LSMO) micro-bridges with thicknesses of 10–100 nm. $La_{0.7}Sr_{0.3}MnO_3$

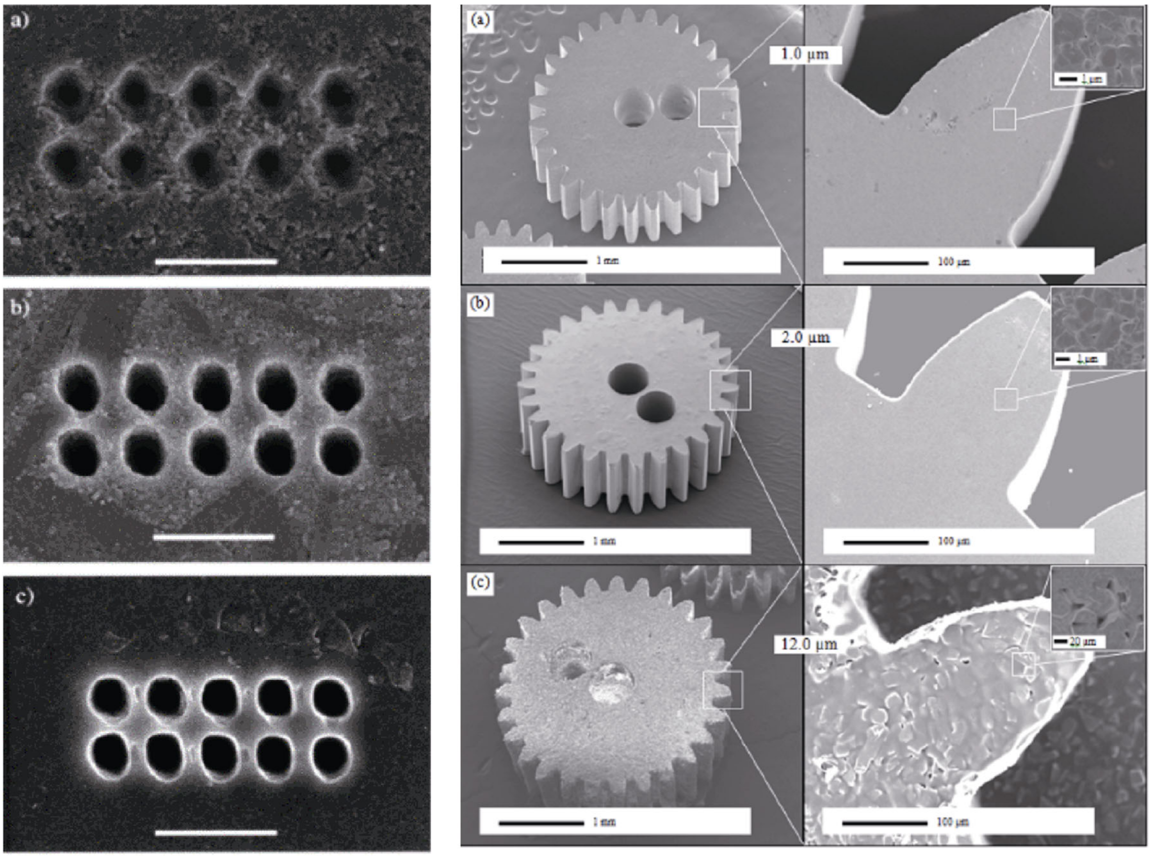

Fig. 24 Ceramic micro holes and micro gears fabricated using soft lithography with different particle sizes. Reproduced with permission from Ref. [171], © Elsevier Ltd. 2015, and Ref. [172], © WILEY-VCH Verlag GmbH 2000.

Table 3 Summary of patterning techniques used for MEMS fabrication

Technique	Shaping	Resolution (μm)	Density	Reference
Micro-injection moulding	Injection, cooling down, ejection, de-binding, sintering	<3	99%	[178]
Micro-electro-phoretic	Deposition of electrically charged particles, sintering	Submicron	99%	[179]
Extrusion	Injection, cooling down, ejection, de-binding, sintering	10	99%	[138]
Soft lithography	Deposition, drying, de-binding, sintering	Submicron	99%	[180]

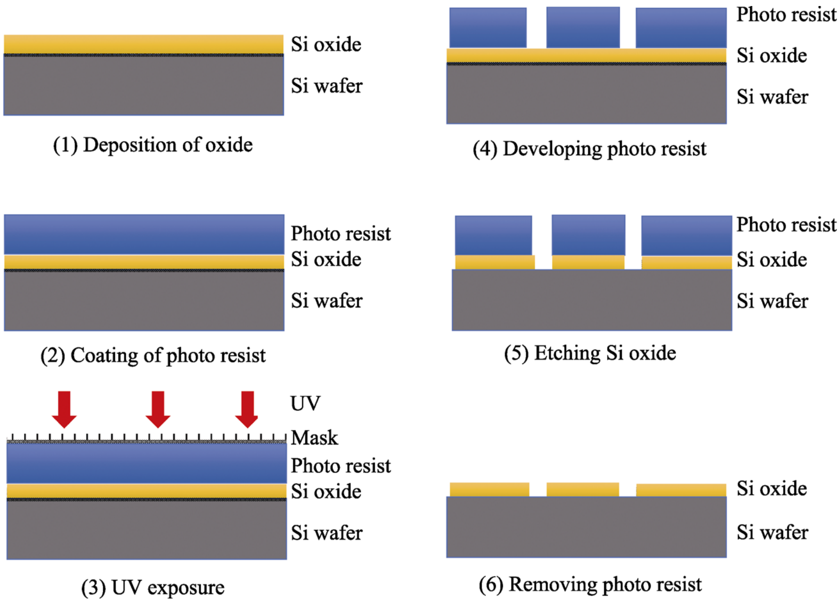

Fig. 25 A schematic diagram of etching micromachining.

layers were grown on $CaTiO_3$ and $SrTiO_3$ on top of a silicon substrate by dry etching. The micro-bridge pattern was first obtained using UV photo-lithography and etched by the ion beam. Next, it was etched using reactive ion (RIE) of SF6 gas. The width of the micro-bridges was 2 and 4 μm while the length was 50–200 μm. The technique is quite popular to develop also moulds for ceramic micro-fabrication and other materials. However, it has also been used to pattern ceramic templates. Piezoelectric ceramic materials have been extensively patterned using a range of etching techniques. Lead zirconate titanate has been a favourite material for various actuation and sensing products such as PZT high-frequency ultrasound transducers as it exhibits low noise, large output signals, and high-frequency operation [184]. Figure 26 shows the top surface and cross-section of PZT etched layer. It can be noted that the surfaces of the samples were uniform and smooth, which confirms that the resolution of etched samples generally outperforms other ceramic microfabrication techniques.

3.3.2 *Micro-electrical discharge machining*

Micro-electrical discharge machining (μEDM) is used to create a wide range of complex shapes. In this process, μEDM machine creates an electrical discharge (the spark) between a workpiece and the electrode to electrically erode the sample, as shown in Fig. 27. There are three processes of micro EDM techniques; hole boring, micro wired EDM, and shaped working

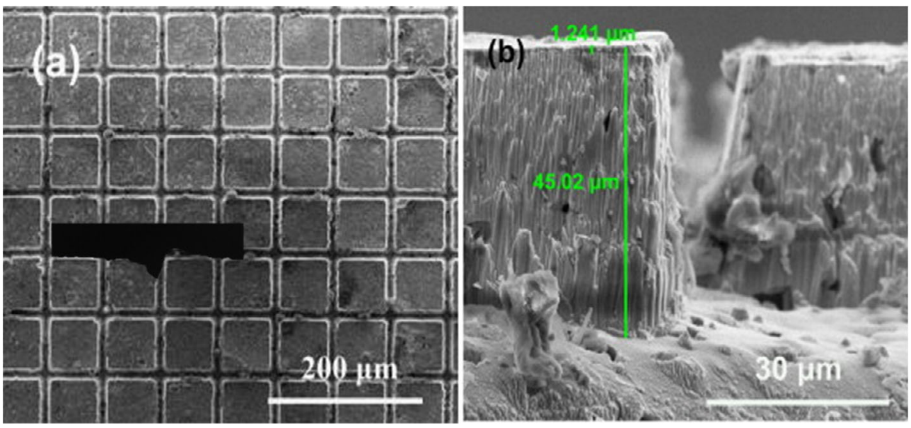

Fig. 26 SEM images of PZT ceramic layer after 7 h etching: (a) top surface, (b) cross section. Reproduced with permission from Ref. [184], © Elsevier Ltd and Techna Group S.r.l. 2015.

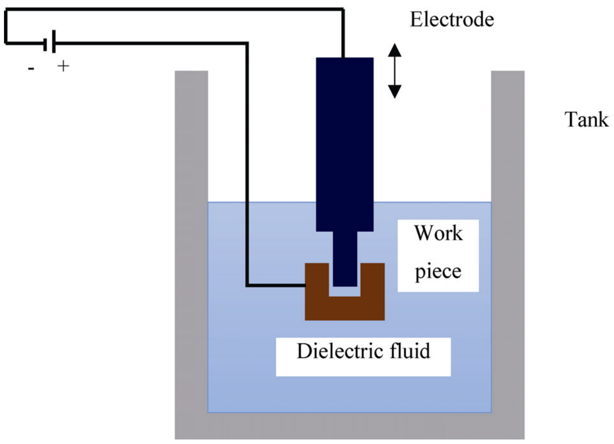

Fig. 27 Schematic diagram of micro-electrical discharge machining (μEDM).

electrode [185]. In hole boring, the electrode is consumed during the process, and hence it is compensated until achieving the required micro features [185,186]. In micro-wire EDM, the electrode is a wire that is drawn continuously during the process to erode the workpiece. The process can produce accurate 3D micro-features of metalwork [187,188]. One of the process limitations is the heat-affected zone of the eroding tool, which degrades the mechanical properties of the affected area [189]. In addition, the process is not suitable for non-conductive materials. Therefore, it is not a popular technique to cut ceramic materials. A conductive silicon carbide seems to be the only ceramic that has been processed using μEDM. Silicon carbide is one of the popular ceramic materials that have many applications. However, it is quite challenging to cut SiC using conventional machining as it has low fracture toughness. Therefore, μEDM offers excellent potentials to machine this material at the micro-level. The operational parameters such as voltage, and threshold on the properties of the sample such as material removal rate, surface roughness, tool wear, radial overcut, and residual stresses can be optimised [190]. Other ceramic materials such as ZrO_2, Si_3N_4, and AlN have been micro-machined using EDM by coating the samples with a conductive layer, assisting electrode, on the surface of the workpiece [191]. The high-energy consumption is one of the issues of cutting non-conductive materials using a conductive coating to break the air gap between the two electrodes. The pulse generator approach is another technique to adjust the voltage of the EDM. It uses an EDM assistant synchronisation servo electrode to cut non-conductive ceramic materials such as Si_3N_4 [192].

3.3.3 Laser micro-machining

Laser micro-machining (LMM), also known as laser ablation, is a technique that utilises a laser beam to pattern micro features on the substrate as depicted in Fig. 28. The foremost benefit of laser micromachining is its suitability to pattern various types of materials. Similar to the micro-EDM technique, LMM can be applied only to thermally conductive materials [193]. Different laser types can be used to process ceramics such as microsecond (Co_2 and Nd:YAG) and excimer lasers. A range of ceramic materials has been processed using laser micro-machining such as alumina, silicon nitride, and aluminium nitride. Devices fabricated using this process include integrated circuits, sensors, micro-cavity structures, transducers, and detectors. Pulsed lasers are the most favourable type in creating patterns in ceramics because they can be well controlled when compared with continuous mode. Laser absorption is the interaction between the laser radiation and the samples, which is a critical phenomenon of the process. It depends on the characteristics of ceramic materials, for instance, the reflection coefficient and the laser wavelength. In addition, the angle between the laser beam and the ceramic surface also affects the laser absorption. Thermal conductivity of ceramics is typically small when compared to metals. Hence, radiation absorption is faster to be converted to heat energy which affects both depths of cavity and machining time. Patterning or ablation is being carried when the applied energy becomes more significant than the material ablation minimum energy. Laser patterning of ceramic materials is generally challenging because of the significant scattering of most of ceramics within the wavelength of the applied laser. Therefore, a combination of short wavelengths and pulses are typically implemented to achieve high-quality patterns. The process also may

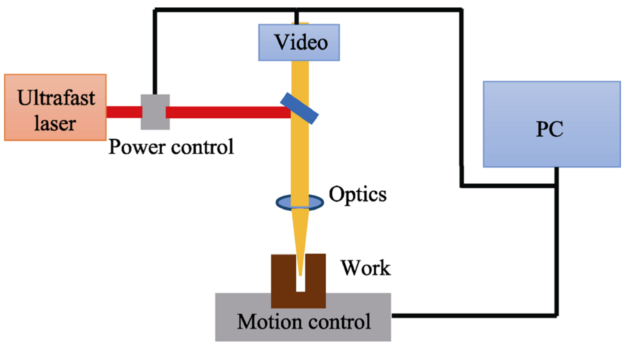

Fig. 28 Schematic diagram of laser micromachining.

exhibit a heat-affected zone which degrades material properties [194–196].

Gai *et al.* [197] studied the influence of scanning velocity and laser pulse energy of a femtosecond laser on the surface quality of silicon carbide. It was found that smooth surface roughness can be achieved at or near the material threshold and that well-defined features can be achieved by several combinations of pulse energies and scanning velocities. Nedialkov *et al.* [198] investigated the use of nanosecond Nd:YAG laser on several ceramic materials such as silicon nitride, aluminium nitride, and alumina using different laser wavelengths. It was concluded that infrared wavelength helped to achieve the best material removal rate. High-quality micro holes of silicon nitride were achieved with respect to the roundness and developed debris when compared to aluminium nitride, and alumina whereas Kim *et al.* [199] created micro-holes with a diameter of 100 μm. Kacar *et al.* [200] studied the effects of Nd:YAG laser power and the duration of the pulse on hole formation drilled on the alumina substrate. Hole crater and exit diameters show a linear proportion when varying the electron power and the duration of the pulse. However, the diameters of the entrance of the hole do not follow the linear trend relationship with the power and the duration of the pulse. This is because the re-solidified materials at the hole entrance are subjected to a higher power and longer pulse duration, which creates a significant material and hence a smaller hole as shown in Fig. 29. A summary table of the subtraction technique is shown in Table 4.

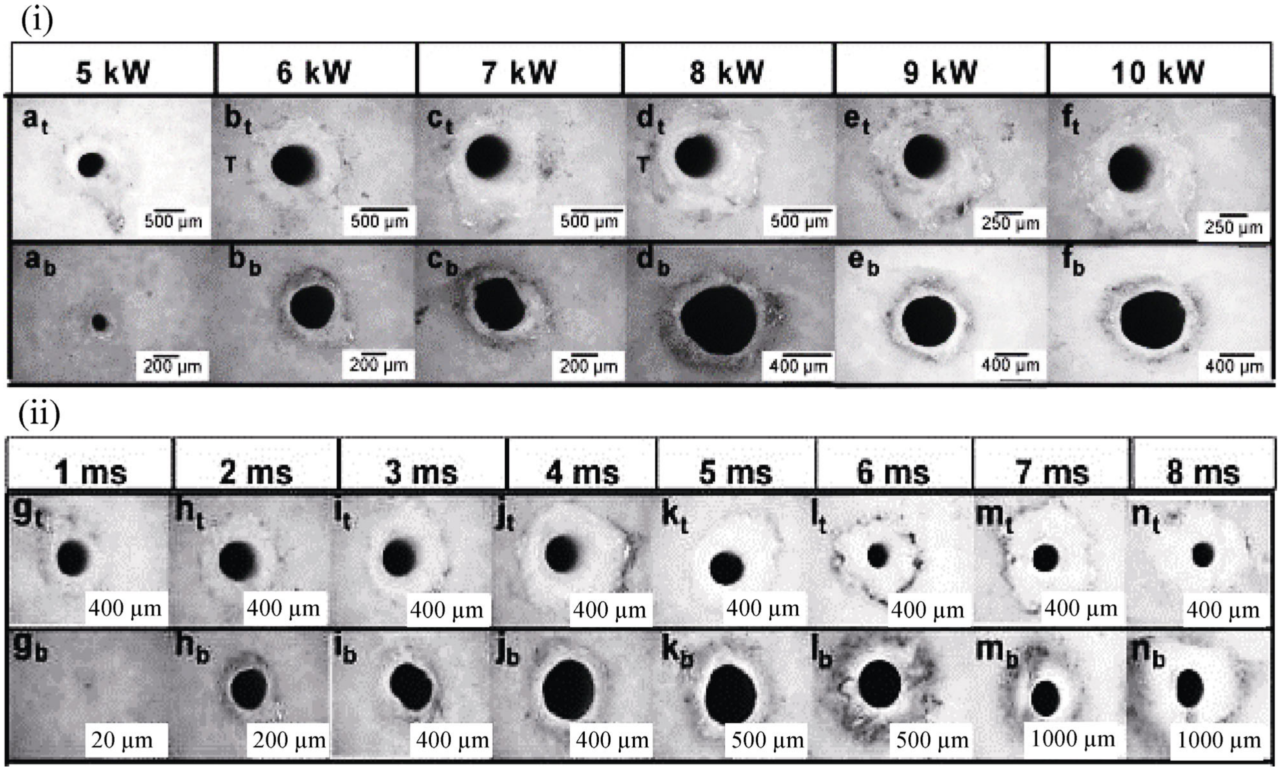

Fig. 29 Optical micro-graphs of holes fabricated using (i) different laser power and (ii) different durations. The first row is the entrance hole while the second row is the exit hole. Reproduced with permission from Ref. [200], © Elsevier B.V. 2008.

Table 4 Summary of subtracting techniques used for MEMS fabrication

Technique	Substracting	Materials	Reference
Etching	Wet, chemical, and physical etching	Conducitive and non-conductive	[201]
Micro-electrical discharge machining	An electrical discharge to erode	Mainly conductive, for non-conductive use of (conductive coatings, pulsing)	[190]
Laser micro machning	A laser beam to pattern	Thermally conductive	[193]

4 Future outlook

The review shows that there is an existing need for complementary ceramic MEMS fabrication techniques that can be carried out without the need for a cleanroom, multiple processing steps, and complex equipment. In addition, there is also a need for on-site and rapid production of free-standing 3D ceramic MEMS with complex shapes. The growing demand for AM technologies, the availability, and low cost of 3D printers, their materials and accessories have triggered AM expansion in wide range applications. As a result, the global market of AM was $1.4 billion in 2010, and it is valued to reach $9 billion in 2019 while it is expected to jump to $35 billion in 2024 (see Fig. 30) [202,203]. There are also significant technical, economic, and environmental benefits of using AM over the traditional micro-fabrication. However, research in using AM of MEMS has not sufficiently matured when compared to the conventional micro-fabrication of ceramic materials, which are relatively well established.

Most additive manufacturing technologies are at their early developmental stages to be real ceramic micro-fabrication techniques. Techniques such as two photons and micro-stereolithography showed a great promise to ceramic microfabrication in terms of maturity and capability while other AM processes such as fused deposition modelling, inkjet printing, and sheet lamination are still lacking. While FDM technology triggered the first wave of awareness and popularity of 3D printing, FDM has not yet fulfilled the required range of technical needs such as surface roughness and the ability to produce micro-features with an adequate resolution for MEMS industries. The poor properties of the FDM printed objects are due to several factors such as the poor adhesion between layers, porosity, or microstructural defects [204]. On the other hand, the roughness is influenced by the layer thickness and the building direction. It is also attributed to the stair-stepping effect, which is caused by the build-up layers. The aforementioned issues can be improved by implementing appropriate post-processing steps. However, post-processing has not yet explored for ceramic micro-fabrication using AM. Figure 31 shows a comparison in the number of publications using micro-stereolithography, two photons, micro injection moulding, deep reactive ion etching, and soft lithography over the last 20 years. The figure shows that two photons and microstereolithography are the most researched and well established for ceramic MEMS development. This is attributed to the fine resolution, material diversity, and the surface roughness which satisfy the requirement of many ceramic MEMS applications. The accuracy and high resolution of micro-stereolithography are attributed to the concept of UV wavelength, which ranges from 10 to 100 nm.

There are still a number of additional challenges that need to address in order to realise a wider adoption of AM. For example, the adhesion of the printed ceramic materials to the typical MEMS substrates such as Si, glass, and SiO_2 needs to be studied, and solutions need to be developed to integrate the 3D printed structures into MEMS devices and to directly print ceramic materials on different wafers.

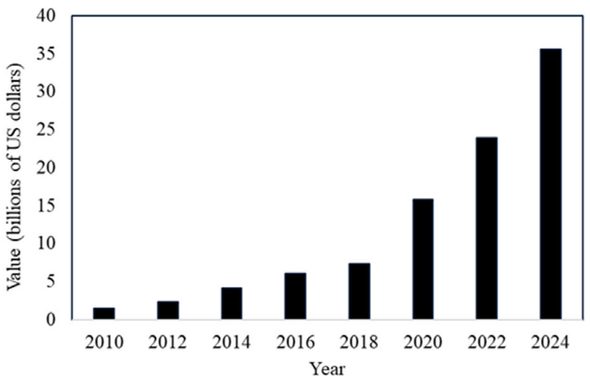

Fig. 30 Revenue growth of AM worldwide from 2010 to 2024.

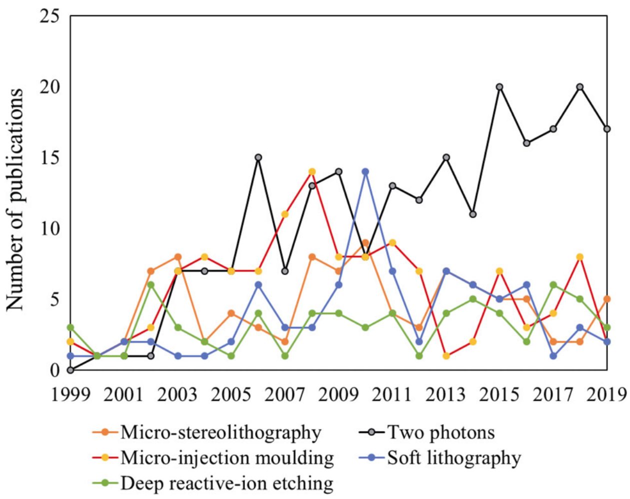

Fig. 31 Number of published papers using micro-stereolithography, two photons, micro injection moulding, deep reactive ion etching, soft lithography over the last 20 years.

5 Conclusions

This paper provided an overview of the state of the art in additive micro-fabrication of ceramic MEMS. The review showed that the advancement in micro-fabrication technologies had been significantly expanding with the introduction of additive manufacturing that enabled rapid and accurate printing of ceramic micro-components. Recently, additive manufacturing has shown a considerable potential to fabricate ceramic MEMS. Applications such as micro-cellular structures for catalyst bed, scaffolds, and micro-sensors have been successfully developed using AM. In particular, AM has managed to transform conventional ceramic foam to more controlled porosity, pore size, and surface area micro-cellular structures. Vat polymerisation, two photons, and micro-stereolithography have been widely investigated to fabricate ceramic micro-components, while proof of concept studies was found for sheet lamination and material jetting. Conventional techniques such as micro-injection moulding, etching, laser micro-machining, and micro-electrical discharge machining are on a slow decline to ceramic MEMS community. On the other hand, there is less interest in using electro-phoretic deposition and extrusion for ceramic micro-fabrication. This is possible because of the geometrical restrictions and need of multi-step production system to achieve the final structures. The review shows that although AM has successfully developed ceramic MEMS, the technique is still facing technical and regulatory challenges. In particular, inherited issues such as internal defects, post-processing, surface roughness, resolution, quality control, and materials recycling as well as printing ceramic on wafers need to be investigated by both additive manufacturing MEMS communities.

References

[1] Essa K, Modica F, Imbaby M, *et al*. Manufacturing of metallic micro-components using hybrid soft lithography and micro-electrical discharge machining. *Int J Adv Manuf Technol* 2017, **91**: 445–452.

[2] Feynman RP. There's plenty of room at the bottom [data storage]. *J Microelectromech Syst* 1992, **1**: 60–66.

[3] Petersen KE. Silicon as a mechanical material. *Proc IEEE* 1982, **70**: 420–457.

[4] Howe RT. Surface micromachining for microsensors and microactuators. *J Vac Sci Technol B* 1988, **6**: 1809.

[5] Brandner JJ. Microfabrication in metals, ceramics and polymers. *Russ J Gen Chem* 2012, **82**: 2025–2033.

[6] Maboudian R. Surface processes in MEMS technology. *Surf Sci Rep* 1998, **30**: 207–269.

[7] Miki N. Techniques in the fabrication of high-speed micro-rotors for MEMS applications. In: *MEMS/NEMS*. Leondes CT, Ed. Boston: Springer, 2006: 335–352.

[8] Hassanin H, Jiang K. Functionally graded microceramic components. *Microelectron Eng* 2010, **87**: 1610–1613.

[9] Zhuiykov S. Development of ceramic electrochemical sensor based on $Bi_2Ru_2O_{7+x}$–RuO_2 sub-micron oxide sensing electrode for water quality monitoring. *Ceram Int* 2010, **36**: 2407–2413.

[10] Bauer W, Müller M, Knitter R, *et al*. Design and prototyping of a ceramic micro turbine: A case study. *Microsyst Technol* 2010, **16**: 607–615.

[11] Bae K, Jang DY, Jung HJ, *et al*. Micro ceramic fuel cells with multilayered yttrium-doped barium cerate and zirconate thin film electrolytes. *J Power Sources* 2014, **248**: 1163–1169.

[12] Zhao R, Shao G, Cao YJ, *et al*. Temperature sensor made of polymer-derived ceramics for high-temperature applications. *Sensor Actuat A: Phys* 2014, **219**: 58–64.

[13] Monri K, Maruo S. Three-dimensional ceramic molding based on microstereolithography for the production of piezoelectric energy harvesters. *Sensor Actuat A: Phys* 2013, **200**: 31–36.

[14] Bystrova S, Luttge R. Micromolding for ceramic microneedle arrays. *Microelectron Eng* 2011, **88**: 1681–1684.

[15] Piotter V, Beck MB, Ritzhaupt-Kleissl HJ, *et al*. Recent developments in micro ceramic injection molding. *Int J Mater Res* 2008, **99**: 1157–1162.

[16] Teterycz H, Kita J, Bauer R, *et al*. New design of an SnO_2 gas sensor on low temperature cofiring ceramics. *Sensor Actuat B: Chem* 1998, **47**: 100–103.

[17] Hassanin H, Jiang K. Fabrication of Al_2O_3/SiC composite microcomponents using non-aqueous suspension. *Adv Eng Mater* 2009, **11**: 101–105.

[18] Liu J, Yang Y, Hassanin H, *et al*. Graphene–alumina nanocomposites with improved mechanical properties for biomedical applications. *ACS Appl Mater Interfaces* 2016, **8**: 2607–2616.

[19] Zhang KQ, Xie C, Wang G, *et al*. High solid loading, low viscosity photosensitive Al_2O_3 slurry for stereolithography based additive manufacturing. *Ceram Int* 2019, **45**: 203–208.

[20] Feng CW, Zhang KQ, He RJ, *et al*. Additive manufacturing of hydroxyapatite bioceramic scaffolds: Dispersion, digital light processing, sintering, mechanical properties, and biocompatibility. *J Adv Ceram* 2020, **9**: 360–373.

[21] Yang LL, Zeng XJ, Ditta A, *et al*. Preliminary 3D printing of large inclined-shaped alumina ceramic parts by direct ink writing. *J Adv Ceram* 2020, **9**: 312–319.

[22] Peng E, Zhang DW, Ding J. Ceramic robocasting: Recent achievements, potential, and future developments. *Adv*

Mater 2018, **30**: 1802404.

[23] Kita J, Dziedzic A, Golonka LJ, *et al*. Properties of laser cut LTCC heaters. *Microelectron Reliab* 2000, **40**: 1005–1010.

[24] Rettig F, Moos R. Ceramic meso hot-plates for gas sensors. *Sensor Actuat B: Chem* 2004, **103**: 91–97.

[25] Iovdalskiy IMOVA, Bleivas IM, Ippolitov VM. Hybrid integrated circuit of gas sensor. 1996.

[26] Suresh A, Mayo MJ, Porter WD, *et al*. Crystallite and grain-size-dependent phase transformations in yttria-doped zirconia. *J Am Ceram Soc* 2003, **86**: 360–362.

[27] Saridag S, Tak O, Alniacik G. Basic properties and types of zirconia: An overview. *World J Stomatol* 2013, **2**: 40–47.

[28] Ghatee M, Shariat MH, Irvine JTS. Investigation of electrical and mechanical properties of 3YSZ/8YSZ composite electrolytes. *Solid State Ionics* 2009, **180**: 57–62.

[29] Butz, B. Yttria-doped zirconia as solid electrolyte for fuel-cell applications. Karlsruher Institut für Technologie, 2009.

[30] Drings H, Brossmann U, Schaefer HE. Preparation of crack-free nano-crystalline yttria-stabilized zirconia. *Phys Stat Sol (RRL)* 2007, **1**: R7–R9.

[31] Capdevila XG, Folch J, Calleja A, *et al*. High-density YSZ tapes fabricated via the multi-folding lamination process. *Ceram Int* 2009, **35**: 1219–1226.

[32] Jardiel T, Sotomayor ME, Levenfeld B, *et al*. Optimization of the processing of 8-YSZ powder by powder injection molding for SOFC electrolytes. *Int J Appl Ceram Technol* 2008, **5**: 574–581.

[33] Cheah KH, Khiew PS, Chin JK. Fabrication of a zirconia MEMS-based microthruster by gel casting on PDMS soft molds. *J Micromech Microeng* 2012, **22**: 095013.

[34] Jiang LD, Cheung R. A review of silicon carbide development in MEMS applications. *Int J Comput Mater Sci Surf Eng* 2009, **2**: 227.

[35] Vasiliev AA, Pisliakov AV, Sokolov AV, *et al.* Non-silicon MEMS platforms for gas sensors. *Sensor Actuat B: Chem* 2016, **224**: 700–713.

[36] Hassanin H, Jiang K. Alumina composite suspension preparation for softlithography microfabrication. *Microelectron Eng* 2009, **86**: 929–932.

[37] Schulz M. Polymer derived ceramics in MEMS/NEMS—a review on production processes and application. *Adv Appl Ceram* 2009, **108**: 454–460.

[38] Brigo L, Schmidt JEM, Gandin A, *et al.* 3D nanofabrication of SiOC ceramic structures. *Adv Sci* 2018, **5**: 1800937.

[39] Schmidt J, Brigo L, Gandin A, *et al*. Multiscale ceramic components from preceramic polymers by hybridization of vat polymerization-based technologies. *Addit Manuf* 2019, **30**: 100913.

[40] Smith GL, Pulskamp JS, Sanchez LM, *et al.* PZT-based piezoelectric MEMS technology. *J Am Ceram Soc* 2012, **95**: 1777–1792.

[41] Gomes C, Greil P, Travitzky N, *et al*. Laminated Object Manufacturing (LOM) of glass ceramics substrates for LTCC applications. In: *Innovative Developments in Design and Manufacturing*. CRC Press, 2009: 239–244.

[42] Yoon YJ, Choi JK, Lim JW, *et al*. Microfluidic devices fabricated by LTCC combined with thick film lithography. *Adv Mater Res* 2009, **74**: 303–306.

[43] Van Tassel JJ, Randall CA. Micron scale conductors and integrated passives in LTCC's by electrophoretic deposition. In: Proceedings of the 1st International Conference and Exhibition on Ceramic Interconnect and Ceramic Microsystems Technologies, 2005: 190–193.

[44] Wilkinson NJ, Smith MAA, Kay RW, *et al*. A review of aerosol jet printing—a non-traditional hybrid process for micro-manufacturing. *Int J Adv Manuf Technol* 2019, **105**: 4599–4619.

[45] Zaraska K, Machnik M, Bieńkowski A, *et al.* Depth of laser etching in green state LTCC. In: Proceedings of the 8th International Conference and Exhibition on Ceramic Interconnect and Ceramic Microsystems Technologies, 2012: 136–141.

[46] Steinhäußer F, Hradil K, Schwarz S, *et al*. Wet chemical porosification of LTCC in phosphoric acid: Celsian forming tapes. *J Eur Ceram Soc* 2015, **35**: 4465–4473.

[47] Rathnayake-Arachchige D, Hutt DA, Conway PP. Excimer laser machining of fired LTCC for selectively metallized open channel structures. *Int Symp Microelectron* 2013, **2013**: 000194–000199.

[48] Canonica MD, Wardle BL, Lozano PC. Micro-patterning of porous alumina layers with aligned nanopores. *J Micromech Microeng* 2015, **25**: 015017.

[49] El-Sayed MA, Hassanin H, Essa K. Effect of casting practice on the reliability of Al cast alloys. *Int J Cast Met Res* 2016, **29**: 350–354.

[50] Hassanin H, Ostadi H, Jiang K. Surface roughness and geometrical characterization of ultra-thick micro moulds for ceramic micro fabrication using soft lithography. *Int J Adv Manuf Technol* 2013, **67**: 2293–2300.

[51] Hassanin H, Ahmed El-Sayed M, ElShaer A, *et al*. Microfabrication of net shape zirconia/alumina nanocomposite micro parts. *Nanomaterials* 2018, **8**: 593.

[52] Thomas P, Levenfeld B, Várez A, *et al*. Production of alumina microparts by powder injection molding. *Int J Appl Ceram Technol* 2011, **8**: 617–626.

[53] Uchikoshi T, Furumi S, Suzuki T, *et al*. Direct shaping of alumina ceramics by electrophoretic deposition using conductive polymer-coated ceramic substrates. *Adv Mater Res* 2007, **29–30**: 227–230.

[54] Shannon T, Blackburn S. The production of alumina/zirconia laminated composites by o-extrusion. In: Proceedings of the 19th Annual Conference on Composites, Advanced Ceramics, Materials, and Structures—B: Ceramic Engineering and Science Proceedings, 1995, **16:** 1115–1120.

[55] Tak HS, Ha CS, Lee HJ, *et al*. Characteristic evaluation of

Al_2O_3/CNTs hybrid materials for micro-electrical discharge machining. *Trans Nonferrous Met Soc China* 2011, **21**: s28–s32.

[56] Hassanin H, Jiang K. Optimized process for the fabrication of zirconia micro parts. *Microelectron Eng* 2010, **87**: 1617–1619.

[57] Rheaume JM, Pisano AP. Surface micromachining of unfired ceramic sheets. *Microsyst Technol* 2011, **17**: 133–142.

[58] Vulcano Rossi VA, Mullen MR, Karker NA, *et al.* Microfabricated electrochemical sensors for combustion applications. In: Proceedings of the SPIE 9491, Sensors for Extreme Harsh Environments II, 2015: 94910J.

[59] Yu PC, Li QF, Fuh JYH, *et al*. Micro injection molding of micro gear using nano-sized zirconia powder. *Microsyst Technol* 2009, **15**: 401–406.

[60] Cao. Growth of oxide nanorod arrays through Sol electrophoretic deposition. *J Phys Chem B* 2004, **108**: 19921–19931.

[61] Zorman CA, Parro RJ. Micro- and nanomechanical structures for silicon carbide MEMS and NEMS. *Phys Stat Sol (b)* 2008, **245**: 1404–1424.

[62] Youn SW, Okuyama C, Takahashi M, *et al*. Replication of nano/micro quartz mold by hot embossing and its application to borosilicate glass embossing. *Int J Mod Phys B* 2008, **22**: 6118–6123.

[63] Chen BK, Zhang Y, Sun Y. Novel mems grippers capable of both grasping and active release of micro objects. In: Proceedings of the 15th International Conference on Solid-State Sensors, Actuators and Microsystems, 2009: 2389–2392.

[64] Yang CT, Ho SS, Yan BH. Micro hole machining of borosilicate glass through electrochemical discharge machining (ECDM). *Key Eng Mater* 2001, **196**: 149–166.

[65] Amnache A, Neumann J, Frechette LG. Capabilities and limits to form high aspect-ratio microstructures by molding of borosilicate glass. *J Microelectromech Syst* 2019, **28**: 432–440.

[66] Gu-Stoppel S, Stenchly V, Kaden D, *et al.* New designs for MEMS-micromirrors and micromirror packaging with electrostatic and piezoelectric drive. *Advanced Manufacturing, Electronics and Microsystems: TechConnect Briefs* 2016, **2016**: 87–90.

[67] Stenchly V, Quenzer HJ, Hofmann U, *et al.* New fabrication method of glass packages with inclined optical windows for micromirrors on wafer level. In: Proceedings of the SPIE 8613, Advanced Fabrication Technologies for Micro/Nano Optics and Photonics VI, 2013: 861319.

[68] Schulz M. Polymer derived ceramics in MEMS/NEMS—A review on production processes and application. *Adv Appl Ceram* 2009, **108**: 454–460.

[69] Tolvanen J, Hannu J, Juuti J, *et al*. Piezoelectric flexible LCP–PZT composites for sensor applications at elevated temperatures. *Electron Mater Lett* 2018, **14**: 113–123.

[70] Gorjan L, Lusiola T, Scharf D, *et al*. Kinetics and equilibrium of eco-debinding of PZT ceramics shaped by thermoplastic extrusion. *J Eur Ceram Soc* 2017, **37**: 5273–5280.

[71] Chen XY, Chen RM, Chen ZY, *et al*. Transparent lead lanthanum zirconate titanate (PLZT) ceramic fibers for high-frequency ultrasonic transducer applications. *Ceram Int* 2016, **42**: 18554–18559.

[72] Montalba C, Ramam K, Eskin DG, *et al*. Fabrication of a novel hybrid AlMg5/SiC/PLZT metal matrix composite produced by hot extrusion. *Mater Des* 2015, **69**: 213–218.

[73] Carponcin D, Dantras E, Michon G, *et al*. New hybrid polymer nanocomposites for passive vibration damping by incorporation of carbon nanotubes and lead zirconate titanate particles. *J Non-Cryst Solids* 2015, **409**: 20–26.

[74] Rai-Choudhury P. *Handbook of Microlithography, Micromachining, and Microfabrication. Volume 1: Microlithography*. SPIE Press, 1997.

[75] Qiu CL, Adkins NJE, Hassanin H, *et al*. *In-situ* shelling via selective laser melting: Modelling and microstructural characterisation. *Mater Des* 2015, **87**: 845–853.

[76] Sabouri A, Yetisen AK, Sadigzade R, *et al*. Three-dimensional microstructured lattices for oil sensing. *Energy Fuels* 2017, **31**: 2524–2529.

[77] Essa K, Jamshidi P, Zou J, *et al*. Porosity control in 316L stainless steel using cold and hot isostatic pressing. *Mater Des* 2018, **138**: 21–29.

[78] Klippstein H, Hassanin H, Diaz de Cerio Sanchez A, *et al*. Additive manufacturing of porous structures for unmanned aerial vehicles applications. *Adv Eng Mater* 2018, **20**: 1800290.

[79] Al-Hashimi N, Begg N, Alany R, *et al*. Oral modified release multiple-unit particulate systems: Compressed pellets, microparticles and nanoparticles. *Pharmaceutics* 2018, **10**: 176.

[80] Mohammed A, Elshaer A, Sareh P, *et al*. Additive manufacturing technologies for drug delivery applications. *Int J Pharm* 2020, **580**: 119245.

[81] Chu GTM, Brady GA, Miao WG, *et al*. Ceramic SFF by direct and indirect stereolithography. *MRS Proc* 1998, **542**: 119.

[82] Ding G, He R, Zhang K, *et al.* Stereolithography-based additive manufacturing of gray-colored SiC ceramic green body. *J Am Ceram Soc* 2019, **102**: 7198–7209.

[83] De Hazan Y, Penner D. SiC and SiOC ceramic articles produced by stereolithography of acrylate modified polycarbosilane systems. *J Eur Ceram Soc* 2017, **37**: 5205–5212.

[84] He RJ, Ding GJ, Zhang KQ, *et al*. Fabrication of SiC ceramic architectures using stereolithography combined with precursor infiltration and pyrolysis. *Ceram Int* 2019, **45**: 14006–14014.

[85] Wang XF, Schmidt F, Hanaor D, *et al*. Additive manufacturing of ceramics from preceramic polymers: A versatile stereolithographic approach assisted by thiol-ene click chemistry. *Addit Manuf* 2019, **27**: 80–90.

[86] Liu W, Wu HD, Tian Z, *et al*. 3D printing of dense structural ceramic microcomponents with low cost: Tailoring the sintering kinetics and the microstructure evolution. *J Am Ceram Soc* 2019, **102**: 2257–2262.

[87] Varadan VK, Varadan VV. Micro stereo lithography for fabrication of 3D polymeric and ceramic MEMS. In: Proceedings of the SPIE 4407, MEMS Design, Fabrication, Characterization, and Packaging, 2001: 147–157.

[88] Zheng X, Lee H, Weisgraber T. Ultralight, ultrastiff mechanical metamaterials. *Science* 2014, **344**: 1373–1377.

[89] Song X, Chen ZY, Lei LW, *et al*. Piezoelectric component fabrication using projection-based stereolithography of barium titanate ceramic suspensions. *Rapid Prototyp J* 2017, **23**: 44–53.

[90] Chen WC, Wang FF, Yan K, *et al*. Micro-stereolithography of KNN-based lead-free piezoceramics. *Ceram Int* 2019, **45**: 4880–4885.

[91] Eckel ZC, Zhou C, Martin JH, *et al.* Additive manufacturing of polymer-derived ceramics. *Science* 2016, **351**: 58–62.

[92] Wang M, Xie C, He R, *et al.* Polymer-derived silicon nitride ceramics by digital light processing based additive manufacturing. *J Am Ceram Soc* 2019, **102**: 5117–5126.

[93] Schmidt J, Colombo P. Digital light processing of ceramic components from polysiloxanes. *J Eur Ceram Soc* 2018, **38**: 57–66.

[94] Schmidt J, Altun AA, Schwentenwein M, *et al*. Complex mullite structures fabricated via digital light processing of a preceramic polysiloxane with active alumina fillers. *J Eur Ceram Soc* 2019, **39**: 1336–1343.

[95] Hatzenbichler M, Geppert M, Gruber S, *et al.* DLP-based light engines for additive manufacturing of ceramic parts. In: Proceedings of the SPIE 8254, Emerging Digital Micromirror Device Based Systems and Applications IV, 2012: 82540E.

[96] Ware HOT, Sun C. Method for attaining dimensionally accurate conditions for high-resolution three-dimensional printing ceramic composite structures using MicroCLIP process. *J Micro Nano-Manuf* 2019, **7**: 031001.

[97] Galatas A, Hassanin H, Zweiri Y, *et al*. Additive manufactured sandwich composite/ABS parts for unmanned aerial vehicle applications. *Polymers* 2018, **10**: 1262.

[98] Klippstein H, Diaz de Cerio Sanchez A, Hassanin H, *et al*. Fused deposition modeling for unmanned aerial vehicles (UAVs): A review. *Adv Eng Mater* 2018, **20**: 1700552.

[99] Huang W, Zhang XL, Wu Q, *et al*. Fabrication of HA/β-TCP scaffolds based on micro-syringe extrusion system. *Rapid Prototyp J* 2013, **19**: 319–326.

[100] Cai K, Román-Manso B, Smay JE, *et al.* Geometrically complex silicon carbide structures fabricated by robocasting. *J Am Ceram Soc* 2012, **95**: 2660–2666.

[101] Touri M, Moztarzadeh F, Osman NAA, *et al*. Optimisation and biological activities of bioceramic robocast scaffolds provided with an oxygen-releasing coating for bone tissue engineering applications. *Ceram Int* 2019, **45**: 805–816.

[102] Colombo P, Schmidt J, Franchin G, *et al.* Additive manufacturing techniques for fabricating complex ceramic components from preceramic polymers. *Am Ceram Soc Bull* 2017, **96**: 16–23.

[103] El-Sayed MA, Essa K, Ghazy M, *et al*. Design optimization of additively manufactured titanium lattice structures for biomedical implants. *Int J Adv Manuf Technol* 2020, **110**: 2257–2268.

[104] Hassanin H, Al-Kinani AA, ElShaer A, *et al*. Stainless steel with tailored porosity using canister-free hot isostatic pressing for improved osseointegration implants. *J Mater Chem B* 2017, **5**: 9384–9394.

[105] Tolipov A, Elghawail A, Abosaf M, *et al*. Multipoint forming using mesh-type elastic cushion: Modelling and experimentation. *Int J Adv Manuf Technol* 2019, **103**: 2079–2090.

[106] Hassanin H, Alkendi Y, Elsayed M, *et al*. Controlling the properties of additively manufactured cellular structures using machine learning approaches. *Adv Eng Mater* 2020, **22**: 1901338.

[107] Cox SC, Jamshidi P, Eisenstein NM, *et al*. Adding functionality with additive manufacturing: Fabrication of titanium-based antibiotic eluting implants. *Mater Sci Eng: C* 2016, **64**: 407–415.

[108] Essa K, Khan R, Hassanin H, *et al*. An iterative approach of hot isostatic pressing tooling design for net-shape IN718 superalloy parts. *Int J Adv Manuf Technol* 2016, **83**: 1835–1845.

[109] Regenfuss P, Streek A, Hartwig L, *et al*. Principles of laser micro sintering. *Rapid Prototyp J* 2007, **13**: 204–212.

[110] Petsch T, Regenfuß P, Ebert R, *et al.* Industrial laser micro sintering. In: Proceedings of the 23rd International Congress on Applications of Laser and Electro-Optics, 2004.

[111] Chen J, Yang J, Zuo T. Micro fabrication with selective laser micro sintering. In: Proceedings of the 1st IEEE International Conference on Nano/Micro Engineered and Molecular Systems, 2006: 426–429.

[112] Streek A, Regenfuß P, Süß T, *et al.* Laser micro sintering of SiO_2 with an NIR-laser. In: Proceedings of the SPIE 6985, Fundamentals of Laser Assisted Micro- and Nanotechnologies, 2008: 69850Q.

[113] Essa K, Hassanin H, Attallah MM, *et al*. Development and testing of an additively manufactured monolithic catalyst bed for HTP thruster applications. *Appl Catal A: Gen* 2017, **542**: 125–135.

[114] Windsheimer H, Travitzky N, Hofenauer A, *et al.* Laminated object manufacturing of preceramic-paper-derived Si–SiC composites. *Adv Mater* 2007, **19**: 4515–4519.

[115] Shama A. *Study of Microfluidic Mixing and Droplet Generation for 3D Printing of Nuclear Fuels*. EPFL, 2017.

[116] Derby B. Inkjet printing of functional and structural materials: Fluid property requirements, feature stability,

and resolution. *Annu Rev Mater Res* 2010, **40**: 395–414.

[117] Derby B. Materials opportunities in layered manufacturing technology. *J Mater Sci* 2002, **37:** 3091–3092.

[118] Zhao XL, Evans JRG, Edirisinghe MJ, *et al*. Direct ink-jet printing of vertical walls. *J Am Ceram Soc* 2002, **85**: 2113–2115.

[119] Hill S. Micromoulding—A small injection of technology. *Mater World* 2001, **9**: 24–25.

[120] Griffiths CA, Dimov SS, Brousseau EB, *et al*. The effects of tool surface quality in micro-injection moulding. *J Mater Process Technol* 2007, **189**: 418–427.

[121] Stone VN, Baldock SJ, Croasdell LA, *et al*. Free flow isotachophoresis in an injection moulded miniaturised separation chamber with integrated electrodes. *J Chromatogr A* 2007, **1155**: 199–205.

[122] Hill SDJ, Kamper KP, Dasbach U, *et al.* An investigation of computer modelling for micro-injection moulding. In: *Simulation and Design of Microsystems and Microstructures*. Southampton, 1995: 275–283.

[123] Liu ZY, Loh NH, Tor SB, *et al.* Micro-powder injection molding. *J Mater Process Technol* 2002, **127**: 165–168.

[124] Loh NH, Tor SB, Tay BY, *et al*. Fabrication of micro gear by micro powder injection molding. *Microsyst Technol* 2007, **14**: 43–50.

[125] Michrafy A, Dodds JA, Kadiri MS. Wall friction in the compaction of pharmaceutical powders: Measurement and effect on the density distribution. *Powder Technol* 2004, **148**: 53–55.

[126] Lee SC, Kim KT. A study on the cap model for metal and ceramic powder under cold compaction. *Mater Sci Eng: A* 2007, **445–446**: 163–169.

[127] Piotter V, Plewa K, Mueller T, *et al*. Manufacturing of high-grade micro components by powder injection molding. *Key Eng Mater* 2010, **447–448**: 351–355.

[128] Attia UM, Alcock JR. Fabrication of ceramic micro-scale hollow components by micro-powder injection moulding. *J Eur Ceram Soc* 2012, **32**: 1199–1204.

[129] Yoo JH, Gao W. Near-net ceramic micro-tubes fabricated by electrophoretic deposition process. *Int J Mod Phys B* 2003, **17**: 1147–1151.

[130] Sarkar P, Prakash O, Wang G, *et al*. Micro-laminate ceramic/ceramic composites (YSZ/Al_2O_3) by electrophoretic deposition. In: Proceedings of the 18th Annual Conference on Composites and Advanced Ceramic Materials—B: Ceramic Engineering and Science Proceedings, 15: 1019–1027.

[131] Von Both H, Dauscher M, Haußelt J. Fabrication of microstructured ceramics by electrophoretic deposition of optimized suspensions. In: Proceedings of the 28th International Conference on Advanced Ceramics and Composites A: Ceramic Engineering and Science Proceedings, 2004: 135–140.

[132] Bonnas S, Ritzhaupt-Kleissl HJ, Haußelt J. Electrophoretic deposition for fabrication of ceramic microparts. *J Eur Ceram Soc* 2010, **30**: 1159–1162.

[133] Laubersheimer J, Ritzhaupt-Kleissl H-J, Hauβelt J, *et al.* Electrophoretic deposition of sol-gel ceramic microcomponents using UV-curable alkoxide precursors. *J Eur Ceram Soc* 1998, **18**: 255–260.

[134] Zaman AC, Üstündağ CB, Kuşkonmaz N, *et al*. 3-D micro-ceramic components from hydrothermally processed carbon nanotube–boehmite powders by electrophoretic deposition. *Ceram Int* 2010, **36**: 1703–1710.

[135] Kastyl J, Chlup Z, Clemens F, *et al*. Ceramic core–shell composites with modified mechanical properties prepared by thermoplastic co-extrusion. *J Eur Ceram Soc* 2015, **35**: 2873–2881.

[136] Soydan AM, Yıldız Ö, Akduman OY, *et al*. A new approach for production of anode microtubes as solid oxide fuel cell support. *Ceram Int* 2018, **44**: 23001–23007.

[137] Sharmin K, Schoegl I. Optimization of binder removal for ceramic microfabrication via polymer co-extrusion. *Ceram Int* 2014, **40**: 3939–3946.

[138] Sharmin K, Schoegl I. Processing and analysis of ceramic mesoscale combustors fabricated by co-extrusion. In: Proceedings of the ASME 2013 International Mechanical Engineering Congress and Exposition. Volume 2A: Advanced Manufacturing, 2013: V02AT02A052.

[139] Powell J, Blackburn S. Co-extrusion of multilayered ceramic micro-tubes for use as solid oxide fuel cells. *J Eur Ceram Soc* 2010, **30**: 2859–2870.

[140] Alexander PW, Brei D, Halloran JW. DEPP functionally graded piezoceramics via micro-fabrication by co-extrusion. *J Mater Sci* 2007, **42**: 5805–5814.

[141] Hoy CV, Barda A, Griffith M, *et al*. Microfabrication of ceramics by Co-extrusion. *J Am Ceram Soc* 2005, **81**: 152–158.

[142] Hassanin H, Jiang K. Net shape manufacturing of ceramic micro parts with tailored graded layers. *J Micromech Microeng* 2014, **24**: 015018.

[143] Brittain S, Paul K, Zhao XM, *et al*. Soft lithography and microfabrication. *Phys World* 1998, **11**: 31–37.

[144] Xia YN, Whitesides GM. Soft lithography. *Annu Rev Mater Sci* 1998, **28**: 153–184.

[145] Rogers JA, Nuzzo RG. Recent progress in soft lithography. *Mater Today* 2005, **8**: 50–56.

[146] Brehmer M, Conrad L, Funk L. New developments in soft lithography. *J Dispers Sci Technol* 2003, **24**: 291–304.

[147] Harris TW. *Chemical Milling*. Oxford: Clarendon Press, 1976.

[148] Wang W, Soper SA. *BioMEMS: Technologies and Applications*. CRC Press, Taylor & Francis Group, LLC, 2007.

[149] Helbert JN. *Handbook of Vlsi Microlithography*. William Andrew Publishing, LLC, Norwich, New York, USA, 2001.

[150] Lorenz H, Despont M, Fahrnl N, *et al.* SU-8: A low-cost negative resist for MEMS. In: Proceedings of the 7th Workshop on Micromachining, Micromechanics and Microsystems in Europe, 1997: 121–124.

[151] Mata A, Fleischman AJ, Roy S. Fabrication of multi-layer SU-8 microstructures. *J Micromech Microeng* 2006, **16**: 276–284.
[152] Roth S, Dellmann L, Racine GA, *et al*. High aspect ratio UV photolithography for electroplated structures. *J Micromech Microeng* 1999, **9**: 105–108.
[153] Bauer W, Knitter R, Emde A, *et al*. Replication techniques for ceramic microcomponents with high aspect ratios. *Microsyst Technol* 2002, **9**: 81–86.
[154] Zhang D, Su B, Button TW. Microfabrication of three-dimensional, free-standing ceramic MEMS components by soft moulding. *Adv Eng Mater* 2003, **5**: 924–927.
[155] Zhang D, Su B, Button TW. Preparation of concentrated aqueous alumina suspensions for soft-molding microfabrication. *J Eur Ceram Soc* 2004, **24**: 231–237.
[156] Kim JS, Jiang K, Chang I. A net shape process for metallic microcomponent fabrication using Al and Cu micro/nano powders. *J Micromech Microeng* 2006, **16**: 48–52.
[157] Imbaby M, Jiang K, Chang I. Fabrication of 316-L stainless steel micro parts by softlithography and powder metallurgy. *Mater Lett* 2008, **62**: 4213–4216.
[158] Hassanin H, Jiang K. Multiple replication of thick PDMS micropatterns using surfactants as release agents. *Microelectron Eng* 2011, **88**: 3275–3277.
[159] Heule M, Schönholzer UP, Gauckler LJ. Patterning colloidal suspensions by selective wetting of microcontact-printed surfaces. *J Eur Ceram Soc* 2004, **24**: 2733–2739.
[160] Lee JH, Hon MH, Chung YW, *et al*. Microcontact printing of organic self-assembled monolayers for patterned growth of well-aligned ZnO nanorod arrays and their field-emission properties. *J Am Ceram Soc* 2009, **92**: 2192–2196.
[161] Nagata H, Ko SW, Hong E, *et al.* Microcontact printed $BaTiO_3$ and $LaNiO_3$ thin films for capacitors. *J Am Ceram Soc* 2006, **89**: 2816–2821.
[162] Zhao XM, Xia YN, Whitesides GM. Fabrication of three-dimensional micro-structures: Microtransfer molding. *Adv Mater* 1996, **8**: 837–840.
[163] Zhang D, Su B, Button TW. Preparation of concentrated aqueous alumina suspensions for soft-molding microfabrication. *J Eur Ceram Soc* 2004, **24**: 231–237.
[164] Moon J, Kang C, Cho S. Microtransfer molding of gelcasting suspensions to fabricate barrier ribs for plasma display panel. *J Am Ceram Soc* 2003, **86**: 1969–1972.
[165] Heule M, Schell J, Gauckler LJ. Powder-based tin oxide microcomponents on silicon substrates fabricated by micromolding in capillaries. *J Am Ceram Soc* 2003, **86**: 407–12.
[166] Heule M, Gauckler LJ. Gas sensors fabricated from ceramic suspensions by micromolding in capillaries. *Adv Mater* 2001, **13**: 1790–1793.
[167] Beh WS, Xia YN, Qin D. Formation of patterned microstructures of polycrystalline ceramics from precursor polymers using micromolding in capillaries. *J Mater Res* 1999, **14**: 3995–4003.
[168] Obreja P, Cristea D, Dinescu A, *et al.* Replica molding of polymeric components for microsystems. In: Proceedings of the 2009 Symposium on Design, Test, Integration & Packaging of MEMS/MOEMS, 2009: 349–352.
[169] Mukherjee R, Patil GK, Sharma A. Solvent vapor-assisted imprinting of polymer films coated on curved surfaces with flexible PVA stamps. *Ind Eng Chem Res* 2009, **48**: 8812–8818.
[170] Lawrence JR, Turnbull GA, Samuel IDW. Polymer laser fabricated by a simple micromolding process. *Appl Phys Lett* 2003, **82**: 4023–4025.
[171] Schönholzer UP, Gauckler LJ. Ceramic parts patterned in the micrometer range. *Adv Mater* 1999, **11**: 630–632.
[172] Schönholzer UP, Hummel R, Gauckler LJ. Microfabrication of ceramics by filling of photoresist molds. *Adv Mater* 2000, **12**: 1261–1263.
[173] Hassanin H, Jiang K. Fabrication and characterization of stabilised zirconia micro parts via slip casting and soft moulding. *Scripta Mater* 2013, **69**: 433–436.
[174] Zhu ZG, Hassanin H, Jiang K. A soft moulding process for manufacture of net-shape ceramic microcomponents. *Int J Adv Manuf Technol* 2010, **47**: 147–152.
[175] Hassanin H, Ostadi H, Jiang K. Surface roughness and geometrical characterization of ultra-thick micro moulds for ceramic micro fabrication using soft lithography. *Int J Adv Manuf Technol* 2013, **67**: 2293–2300.
[176] Hassanin H, Jiang K. Net shape manufacturing of ceramic micro parts with tailored graded layers. *J Micromech Microeng* 2014, **24**: 015018.
[177] Hassanin H, Jiang K. Infiltration-processed, functionally graded materials for microceramic componenets. In: Proceedings of the 2010 IEEE 23rd International Conference on Micro Electro Mechanical Systems, 2010: 368–371.
[178] Piotter V, Bauer W, Knitter R, *et al*. Powder injection moulding of metallic and ceramic micro parts. *Microsyst Technol* 2011, **17**: 251–263.
[179] Corni I, Ryan MP, Boccaccini AR. Electrophoretic deposition: From traditional ceramics to nanotechnology. *J Eur Ceram Soc* 2008, **28**: 1353–1367.
[180] Ten Elshof JE, Khan SU, Göbel OF. Micrometer and nanometer-scale parallel patterning of ceramic and organic–inorganic hybrid materials. *J Eur Ceram Soc* 2010, **30**: 1555–1577.
[181] Chang YF, Chou QR, Lin JY, *et al*. Fabrication of high-aspect-ratio silicon nanopillar arrays with the conventional reactive ion etching technique. *Appl Phys A* 2006, **86**: 193–196.
[182] Sammak A, Azimi S, Izadi N, *et al*. Deep vertical etching of silicon wafers using a hydrogenation-assisted reactive ion etching. *J Microelectromech Syst* 2007, **16**: 912–918.
[183] Liu S, Guillet B, Adamo C, *et al*. Free-standing $La_{0.7}Sr_{0.3}MnO_3$ suspended micro-bridges on buffered silicon substrates showing undegraded low frequency noise properties. *J Micromech Microeng* 2019, **29**:

065008.

[184] Zhang JS, Ren W, Jing XP, *et al*. Deep reactive ion etching of PZT ceramics and PMN-PT single crystals for high frequency ultrasound transducers. *Ceram Int* 2015, **41**: S656–S661.

[185] Chow HM, Yan BH, Huang FY. Micro slit machining using electro-discharge machining with a modified rotary disk electrode (RDE). *J Mater Process Technol* 1999, **91**: 161–166.

[186] Weng FT, Shyu RF, Hsu CS. Fabrication of micro-electrodes by multi-EDM grinding process. *J Mater Process Technol* 2003, **140**: 332–334.

[187] Chen ST. Fabrication of high-density micro holes by upward batch micro EDM. *J Micromech Microeng* 2008, **18**: 085002.

[188] Egashira K, Mizutani K. Micro-drilling of monocrystalline silicon using a cutting tool. *Precis Eng* 2002, **26**: 263–268.

[189] Phatthanakun R, Songsiriritthigul P, Klysubun P, *et al.* Multi-step powder casting and X-ray lithography of SU-8 resist for complicated 3D microstructures. In: Proceedings of the 2008 5th International Conference on Electrical Engineering/Electronics, Computer, Telecommunications and Information Technology, 2008: 805–808,

[190] Saxena KK, Agarwal S, Khare SK. Surface characterization, material removal mechanism and material migration study of micro EDM process on conductive SiC. *Procedia CIRP* 2016, **42**: 179–184.

[191] Ojha N, Zeller F, Müller C, *et al*. Comparative study on parametric analysis of μEDM of non-conductive ceramics. *Key Eng Mater* 2014, **611–612**: 693–700.

[192] Zhang HF, Liu YH, Chen JM, *et al*. Experimental research on pulse generator for EDM of non-conductive ceramics. *Key Eng Mater* 2009, **407–408**: 649–653.

[193] Pallav K, Ehmann KF. Feasibility of laser induced plasma micro-machining (LIP-MM). In: *Precision Assembly Technologies and Systems. IFIP Advances in Information and Communication Technology, Vol. 315*. Ratchev S, Ed. Springer Berlin Heidelberg, 2010: 73–80.

[194] Chen J, Yin Y. Laser micro-fabrication in RF MEMS switches. In: Proceedings of the 2009 13th International Symposium on Antenna Technology and Applied Electromagnetics and the Canadian Radio Sciences Meeting, 2009: 1–5.

[195] Amer MS, Dosser L, LeClair S, *et al*. Induced stresses and structural changes in silicon wafers as a result of laser micro-machining. *Appl Surf Sci* 2002, **187**: 291–296.

[196] Amer MS, El-Ashry MA, Dosser LR, *et al*. Femtosecond versus nanosecond laser machining: Comparison of induced stresses and structural changes in silicon wafers. *Appl Surf Sci* 2005, **242**: 162–167.

[197] Rihakova L, Chmelickova H. Laser micromachining of glass, silicon, and ceramics. *Adv Mater Sci Eng* 2015, **2015**: 1–6.

[198] Knowles MRH, Rutterford G, Karnakis D, *et al*. Laser micro-milling of ceramics, dielectrics and metals using nanosecond and picosecond lasers. In: Proceedings of the 4M 2006 - Second International Conference on Multi-Material Micro Manufacture, 2006: 131–134.

[199] Kim SH, Balasubramani T, Sohn I-B, *et al.* Precision microfabrication of AlN and Al_2O_3 ceramics by femtosecond laser ablation. In: Proceedings of the SPIE 6879, Photon Processing in Microelectronics and Photonics VII, 2008: 68791O.

[200] Kacar E, Mutlu M, Akman E, *et al*. Characterization of the drilling alumina ceramic using Nd:YAG pulsed laser. *J Mater Process Technol* 2009, **209**: 2008–2014.

[201] Ferraris E, Vleugels J, Galbiati M, *et al.* Investigation of micro electrical discharge machining (EDM) performance of TiB_2. In: Proceedings of the 16th International Symposium on Electromachining, 2010: 555–560.

[202] Wohlers T, Caffrey T, Campbell RI, *et al. Wohlers Report 2018: 3D Printing and Additive Manufacturing State of the Industry; Annual Worldwide Progress Report*. Wohlers Associates, 2018.

[203] Caffrey T. *Wohlers Report 2015: Additive Manufacturing and 3D Printing*. State of the Industry, Ft. Collins, CO: Wohlers Associates, 2015.

[204] Licciulli A, Esposito Corcione C, Greco A, *et al*. Laser stereolithography of ZrO_2 toughened Al_2O_3. *J Eur Ceram Soc* 2005, **25**: 1581–1589.